Selective activation of Unfolded Protein Response (UPR) by herpes simplex virus type 1 (HSV-1) in permissive and non permissive cells

A Thesis submitted to the College of Graduate Studies and Research in Partial Fulfillment for the requirements for the Degree of Master of science in the Department of Veterinary Microbiology, University of Saskatchewan, Saskatoon

By
Iran Yousefi

Permission to use

In presenting this thesis in partial fulfillment of the requirements for a Postgraduate degree from the University of Saskatchewan, I agree that the Libraries of this University may make if freely available for inspection. I further agree that permission for copying of this thesis in any manner, in whole or in part, for scholarly purpose may be granted by the professor or professors who supervised my thesis work or, in their absence, by the Head of the Department or the Dean of the College in which my work was done. It is understood that any copying or publication or use of this thesis or part thereof for financial gain shall not allowed without my written permission. It is also understood that due recognition shall be given to me and to the University of Saskatchewan in any scholarly use which may be made of any material in my thesis.

Request for permission to copy or to make other use of material in this thesis in whole or part should be addressed to:

Head of the Department of Veterinary Microbiology
University of Saskatchewan
52 Campus Drive
Saskatoon, Saskatchewan S7N 5B4

Abstract

The unfolded protein response (UPR) is induced by a variety of external and internal stimuli, including accumulation of misfolded proteins in the endoplasmic reticulum (ER). Viruses such as Herpes Simplex Virus type 1 (HSV-1) induce host cells to produce viral proteins many of which undergo glycosylation and other modifications in the ER, causing stress to the ER and consequently UPR activation. I have tested the hypothesis that HSV-1 has evolved strategies to regulate the UPR in order to suppress aspects of the UPR that might interfere with viral replication and to promote pathways that aid its own survival and replication.

The purpose of this study was to test the hypothesis that HSV-1 selectively modulates the three pathways (PERK, ATF6, and IRE-1) of the UPR in epithelial and neuronal cells and to examine the similarities and the differences between these two types of cells in their responses to ER stress. Vero and ONS-76 cells were used as models of epithelial and neuronal cells respectively and qRT PCR technique was used for analyzing RNA levels of transcripts of spliced Xbp1, HERP, CHOP and BIP, selected target genes for three pathways of the UPR.

HSV-1 DNA synthesis and infectious virus production in infected cells showed that compared to the permissive Vero cells, ONS-76 cells seemed to be semi-permissive to HSV-1 infection with limited viral DNA synthesis and infectious virus production.

The kinetics of transcript and protein synthesis for genes representing immediate early, early and late classes of viral genes was also monitored. Expression of the immediate early gene, ICP0, was similar in both cell types but the expression of the early gene, TK and late genes VP16 and VP 5 was different.

My work reveals that HSV-1 infection in cells of epithelial and neuronal origins results in activation of the UPR, but through cell type selective regulation of the three signal transduction pathways of the UPR (PERK, ATF6, and IRE-1). While HSV-1 infection resulted in upregulation of Spliced Xbp1 and its target gene HERP (IRE1 pathway) and downregulation of BIP (ATF6 pathway) in both cell types, CHOP (PERK pathway) was upregulated only in ONS cells. My results suggest that some aspects of the UPR are regulated differently in cells

representing the sites for HSV-1 lytic and latent infections. This may indicate the need for increasing the capacity for protein folding and degradation (Xbp1 and ATF6-induced) in both cells but a requirement for suppressing apoptosis (PERK-induced) only in epithelial cells.

As well, I show that HSV-1 infection not only selectively activates the UPR pathways in different cell types, but also inactivates some components of the UPR pathways activated by the drug thapsigargin.

Acknowledgments

This thesis would not have been possible without the guidance and the help of several individuals who in one way or another contributed and extended their valuable assistance in the preparation and completion of this study.

First I would like to express my appreciation to my supervisor Dr. Vikram Misra for his guidance, mentorship and technical expertise. I express my gratitude to Dr. Janet Hill for listening to me when things were difficult and providing me with her valuable advice. I offer my regards and appreciation to other members of my committee for their time and guidance: Dr. Joyce Wilson, Dr. Suresh Tikoo, and Dr. Valerie Verge.

Special thanks to the members of my laboratory, Noreen for her technical assistance, Tim and 2010 summer students for their friendship. To Bonnie for her constant support and guidance and Champika for her willingness to help. To the graduate students and staff of the Department of Veterinary Microbiology, GMP, secretary office. To Azalea Barrieses for her passion for teaching academic English writing.

A thank and gratitude to my family for their understanding, endless love and patience through my study.

Table of Contents

PERMISSION TO USE ..... **I**

ABSTRACT ..... **II**

ACKNOWLEDGMENTS ..... **IV**

LIST OF FIGURES ..... **VII**

LIST OF TABLES ..... **VIII**

CHAPTER 1: INTRODUCTION **1**

1.1. UNFOLDED PROTEIN RESPONSE **1**

1.1.1. ENDOPLASMIC RETICULUM (ER) 1

1.1.2. ER STRESS 2

1.1.3. THE UNFOLDED PROTEIN RESPONSE 2

1.1.4. IRE1 3

1.1.5. PERK 6

1.1.6. ACTIVATING TRANSCRIPTION FACTOR 6 (ATF6) 9

1.1.7. VIRUSES AND UPR 9

1.1.8. HSV AND UPR 13

1.2. HERPES SIMPLEX VIRUS-1 (HSV-1) **14**

1.2.1. THE *HERPESVIRIDAE* FAMILY 14

1.2.2. HSV-1 LYTIC AND LATENT INFECTION 14

1.2.3. HSV VIRUS STRUCTURE 15

1.2.3.1. Core *15*

1.2.3.2. Tegument *15*

1.2.3.3. Capsid *15*

1.2.3.4. Envelope *15*

1.2.4. VIRAL GENES REGULATION DURING LYTIC INFECTION 16

1.2.4.1. IE, E, L genes *16*

1.2.4.2. Initiation of the lytic cycle by VP16, Host Cell Factor and Oct-1 ..... *16*

1.2.5. LATENT INFECTION 17

1.2.5.1. Latency establishment and maintenance *17*

1.2.5.2. HSV-1 reactivation from latency *18*

1.2.5.3. Neuronal model of HSV-1 infection *19*

1.3. HYPOTHESIS **20**

1.3.1 Main objective *20*

1.3.2. Specific objectives: *20*

1.3.2.1. To establish the time course of various parameters of viral replication in Vero (epithelial) and ONS-76 (neuronal) cells. *20*

1.3.2.2. To evaluate the efficiency of the primers designed to quantify the transcription of genes representative the three arms of UPR (IRE1, PERK, ATF6) *20*

1.3.2.3. To determine if expression of the genes representing of the three main pathways of UPR are affected during infection with HSV-1 ..... *20*

1.3.2.4. To study if HSV-1 can selectively inactivate components of the UPR *21*

1.3.2.5. To determine if ICP0 or VP16 viral genes are required to shut off the UPR *21*

CHAPTER 2: MATERIAL AND METHODS **22**
2.1. CELL CULTURE 22
2.2. VIRUS 22
2.3. SINGLE-STEP GROWTH CURVE 22
2.4. PLAQUE ASSAY 23
2.5. DNA PURIFICATION AND ANALYSIS 23
2.6. RNA PURIFICATION AND REAL TIME PCR (QRT PCR) ANALYSIS 23
2.7. WESTERN BLOT ANALYSIS 26
2.8. CELL VIABILITY 27
2.9. PLASMIDS 27
2.10. IMMUNOFLUORESCENCE 27
CHAPTER 3: RESULTS **29**
3.1. KINETICS OF VARIOUS PARAMETERS OF HSV-1 VIRAL INFECTION IN VERO AND ONS-76 CELLS 29
3.1.1 Kinetics of DNA synthesis and infectious virus multiplication in Vero and ONS-76 cells *29*
3.1.2. Kinetics of viral RNA expression in HSV-1 infected ONS-76 and Vero cells *31*
3.1.3. Viral protein synthesis in Vero and ONS-76 cells *37*
3.2. UPR 39
3.2.1. Viability of cells following thapsigargin treatment *39*
3.2.2. Evaluate the efficiency of the primers designed to quantify the transcription of genes representative the three arms of UPR (IRE1, PERK, ATF6) *41*
3.2.3. HSV-1 induces the UPR *43*
3.2.4. HSV-1 infection does not inhibit eIF2α phosphorylation in Vero cells *45*
3.2.6. Transient expression of ICP0 or VP16 does not increase Xbp1 spliced, CHOP and BIP expression *49*
CHAPTER 4: DISCUSSION **51**
REFERENCES: **56**

List of Figures

Figure		Page
Figure 1.1	Schematic illustration of the Unfolded Protein response	4
Figure 1.2	Xbp1 splicing	5
Figure 1.3	eIF2 and protein synthesis	7
Figure 1.4	ATF4	8
Figure 1.5	ATF6	11
Figure 3.1.1	Time course of DNA synthesis and infectious virus production in HSV-1 infected Vero and ONS-76 cells	30
Figure 3.1.2	ICP0, TK, VP16 and VP5 genes expression in HSV-1 infected Vero and ONS-76 cells	32
Figure 3.1.3	Effect of HSV-1 infection on GAPDH expression	34
Figure 3.1.4	Cyclohexamide inhibits the expression of VP16 in both Vero and ONS-76 cells	36
Figure 3.1.5	Kinetics of HSV-1 Protein synthesis in Vero and ONS-76 cells	38
Figure 3.2.1	Thapsigargin and DMSO had no cytotoxicity effect on Vero cells	40
Figure 3.2.2	Expression of UPR- regulated genes in Vero and ONS cells in response to thapsigargin	42
Figure 3.2.3	HSV-1 selectively activate the three arms of the UPR	44
Figure 3.2.4	HSV-1 infection does not inhibit eIF2α phosphorylation in Vero cells but inhibits it in ONS-76 cells	46
Figure 3.2.5	HSV-1 can selectively inactivate components of the UPR	48
Figure 3.2.6	ICP0 and VP16 transient expression did not activate UPR components, Xbp-1 S, CHOP and BIP	50

List of Tables

Table	**Page**
Table 2.1	25
Table 3.1	32

List of Abbreviations

ATF4	Activation transcription factor 4
ATF6	Activation transcription factor 6
Bcl-2	B-cell lymphoma 2
BH3	Bcl-2 homology 3
BIP	Immunoglobulin binding protein
Bp	Base pair
cAMP	Cyclic adenosine monophosphate
CHOP	C/EBP homologous protein
CMV	Cytomegalovirus
CREB3	Cyclic AMP-responsive element binding protein 3
Ct	Cycle threshold
CVB3	Coxsackievirus B3
DMEM	Dulbecco's Modified Eagle Medium
DMSO	Dimethyl sulfoxide
DNA	Deoxyribonucleic acid
DRG	Dorsal root ganglia
E	Early
EBV	Epstein-Barr virus
eIF2	Eukaryotic translation initiation factor
ER	Endoplasmic reticulum
ERAD	ER-associated degradation
EROL1	ER oxidoreduction1 like protein
ERp29	Endoplasmic reticulum protein 29
ERSE	ER responsive elements
GADD34	Growth arrest and DNA damage protein 34
GRP78	Glucose Regulated Protein 78
GRP94	Glucose Regulatory Protein 94
GDP	Guanosine diphosphate

GTP	Guanosine triphosphate
HBx	Hepatitis B virus regulatory x protein
HCF	Host cell factor
HCV	Hepatitis C virus
HCMV	Human Cytomegalovirus
HERP	Homocysteine-induced ER protein
HHV	Human herpes virus
Hsp70	Heat shock protein
HSV-1	Herpes simplex virus type 1
HSV-2	Herpes simplex virus type 2
ICP	Infected cell protein
IE	Immediate early
IMR32	Human neuroblastoma
IRE1	Inositol requiring enzyme1
JNK	c-Jun-N terminal kinase
L	Late
LAT	latency associated transcripts
LCMV	Lymphotic choriomeningitis virus
Met	Methionyl
MOI	Multiplicity of infection
miRNA	micro RNA
NGF	Nerve growth factor
NLS	Nuclear localization signal
Oct1	Octamer binding protein 1
ONS-76	Human medulloblastoma cells
ORF	Open reading frame
PC12	Rat phaeochromocytoma cells
PCR	Polymerase chain reaction
PDI	Protein disulfate isomerase
PERK	Protein kinase R (PKR)- like ER kinase
PFU	Plaque forming unit

PKR	Protein kinase R
PBS	Phosphate buffer saline
PP1	Protein phosphatase 1
Q TR PCR	Real time polymerase chain reaction
RNA	Ribonucleic acid
S1P, S2P	Site 1 and 2 proteases
SDS	Sodium dodecyl sulfate
SDS PAGE	SDS-polyacrylamide gel electrophoresis
SREBP1	Sterol regulatory element-binding protein 1
TK	Thymidine kinase
UPR	Unfolded protein response
VHS	Virus host shut off protein
VP	Virion protein
VP16	Virion transactivator factor 16
VZV	Varicella-zoster virus
Xbp1	Transcriptional factor Xbp1

CHAPTER 1: Introduction

1.1. Unfolded Protein Response

1.1.1. Endoplasmic reticulum (ER)

The endoplasmic reticulum (ER) is a large network of folded membranes present throughout cytoplasm. It extends from the cell membrane through the cytoplasm to the nuclear membrane. It has an important role in the biosynthesis, assemble, glycosylation, folding and transport of proteins and lipids, which are destined for insertion in the cell membrane or for secretion to the outside of the cell. The internal compartment of the ER (lumen) collects proteins synthesized in the cytoplasm for modification and delivery to the secretory pathway (reviewed in 38, 56).

The ER takes two forms, rough (granular) with ribosomes associated with the outer surface, and smooth (with no ribosomes attached). The rough endoplasmic reticulum is involved mainly with the production and processing of proteins that will be exported, or secreted from the cell. The ribosomes assemble amino acids into protein units, which are transported into the rough endoplasmic reticulum for further processing. These proteins may be either transmembrane proteins, which become inserted in the membrane of the endoplasmic reticulum, or water-soluble proteins, which are able to pass completely through the membrane into the lumen of ER. In ER, these proteins are folded into their required three-dimensional conformation and undergo posttranslational modification important for their final structure and function. Modifiers, such as carbohydrates or sugars are added, then the ER either transports the completed proteins to areas of the cell where they are needed, or they are sent to the Golgi apparatus for further processing and modification.

The smooth ER is involved in the synthesis of lipids, metabolism of carbohydrates, calcium homeostasis and detoxification of some toxic chemicals (reviewed in 23, 38, 56). It is also involved in the transport of the products of rough ER to Golgi apparatus. Protein folding is the post-translational process by which a polypeptide folds into its characteristic and functional (native) three-dimensional structure (reviewed in 23, 38, 56).

Since proper folding is essential for protein function, the ER has a quality control system

that identifies misfolded or unfolded proteins, transports them into the cytosol and finally labels them for degradation through the ER-associated degradation process (ERAD). Thus, any harmful effects that these protein might have are limited (reviewed in 31). This quality control process is supported and monitored by ER chaperones and folding enzymes including, the protein disulfate isomerase (PDI), endoplasmic reticulum protein 29 (ERp29), the 70 kilodalton heat shock protein (Hsp70) family member 78 kDa glucose-regulated protein (Grp78), calnexin, calreticulin, and the peptidylpropyl isomerase family. Therefore, only properly-folded proteins are transported from the rough ER to the Golgi complex (reviewed in 55).

1.1.2. ER stress

ER stress involves all the conditions that interfere with the function of ER. ER provides an environment for the production of secretory and membrane proteins. Almost 30% of newly synthesized proteins are rapidly degraded perhaps due to improper protein folding (reviewed in 69). Even a temporary increase in the translation of secretory proteins may cause an accumulation of misfolded proteins. The situation becomes worse if the ER environment is disturbed following conditions such as change in redox state and calcium levels, or failure in the secretory proteins modification (reviewed in 45). Following conditions such as glucose deprivation, hypoxia, dysregulation of calcium homeostasis (i.e. treatment with thapsigargin a chemical compound that can disrupt calcium homeostasis through inhibition of the ER Ca2+-ATPase pump (SERCA), resulting in depletion of ER Ca2+ stores) and excessive protein traffic (i.e. such as occurs with HSV-1 infection), unfolded or misfolded proteins accumulate in the lumen of ER and cause ER stress (reviewed in 38).

1.1.3. The Unfolded Protein Response

The unfolded protein response (UPR) is the mechanism by which cells sense and respond to excess of unfolded or misfolded proteins in the ER. The UPR has a critical role in maintaining cellular functions under ER stress (reviewed in 53). The UPR triggers signaling pathways which have several goals: increasing the folding capacity of the ER by transcriptional activation of molecular chaperones and folding enzymes, decreasing the folding demand through downregulating gene transcription and protein synthesis, and finally increasing clearance of the misfolded or unfolded proteins through ER-associated degradation (ERAD) (reviewed in 68). The UPR signals through three proximal stress sensors located at the ER membrane; inositol

requiring enzyme1 (IRE1), protein kinase R (PKR)- like ER kinase (PERK) and activation transcription factor 6 (ATF6) (reviewed in 20, 38) also see Figure 1). In non-stressed conditions the three sensors of the UPR are suppressed by immunoglobulin binding protein (BIP) also known as Glucose Regulated Protein 78 (GRP78) (reviewed in 20, 38, 55). Following accumulation of unfolded proteins and leading to ER stress, BIP is released from the sensors, IRE1, PERK and ATF6 and then binds to unfolded proteins. Upon the release of BIP, the three sensors trigger a complex cascade of signals resulting in the activation of downstream UPR related genes (1, 4, 5) Figure 1.1.

1.1.4. IRE1

On activation of the UPR, BIP release allows IRE1 dimerizartion and trans-autophosphorylation which activates its endoribonuclease activity and initiates splicing of the mRNA encoding the transcriptional factor Xbp1 (Xbp1 U). Activated IRE1 removes a 26 nucleotide intron from the Xbp1 transcript that, results in a frame shift at codon 165. Splicing of Xbp1 mRNA causes the removal of the 3'-terminal 97 codons from open reading frame (ORF) 1 and addition of the 212 codon ORF 2 to the 5' terminal 164 codons containing the b zip domain (89)(Figure 1.2). The spliced mRNA is called Xbp1 S.

Xbp1 S is translated and transported to the nucleus where it upregulates the expression of the genes that are required to relieve ER stress. These include genes that are involved in protein folding, protein entry to the ER and ERAD (reviewed in 23, 29, 38, 68). Prolonged UPR activation leads to apoptotic cell death. In such an event, activation of IRE1 activates apoptosis signal-regulating kinase 1 (ASK 1), c-Jun-N terminal kinase (JNK) and mitogen activated protein kinase (p38)(29).

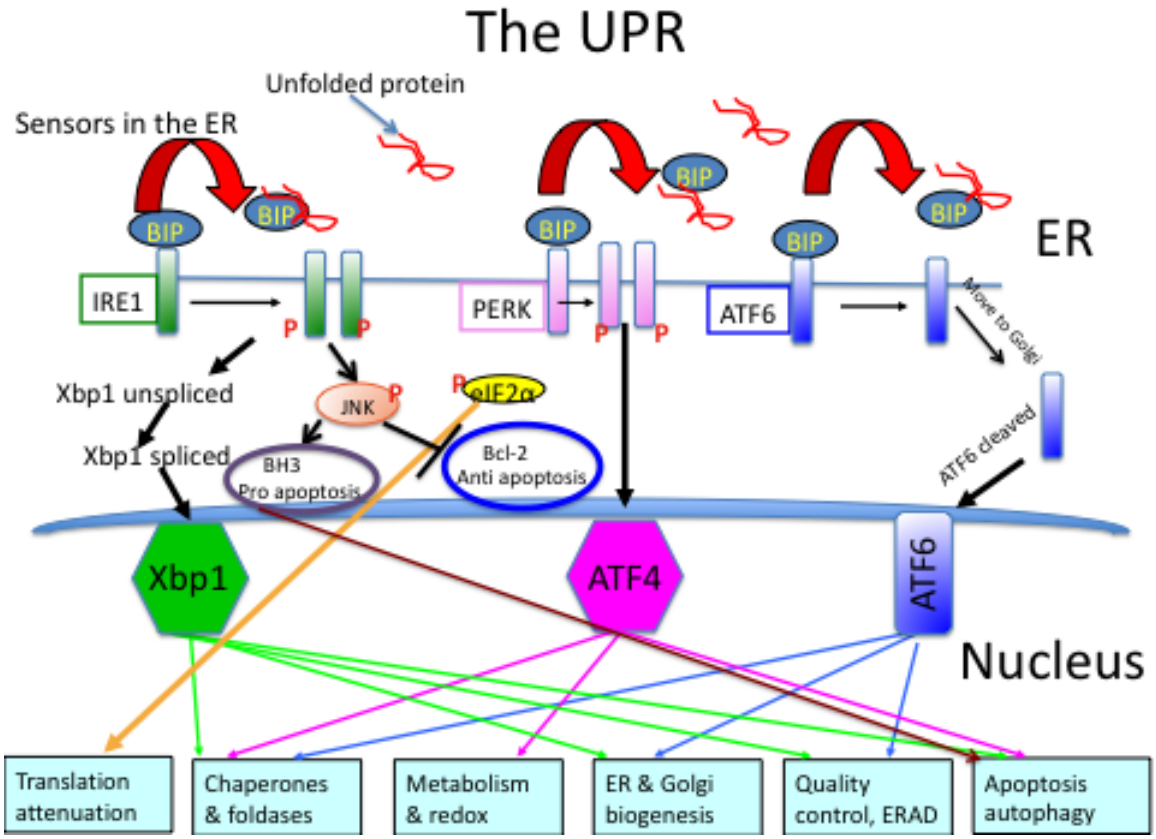

Figure 1.1 Schematic illustration of the Unfolded Protein Response. Three transmembrane sensors, IRE1, PERK and ATF6 are negatively regulated by binding to Immunoglobulin Binding Protein (BIP). Accumulation of unfolded or misfolded proteins leads to ER stress and the release of BIP from these sensors. IRE1 detachment from BIP allows its dimerization, autophoshorylation and activates its endoribouclease activity, which results in the splicing of Xbp1 mRNA. Xbp1 protein synthesized from the spliced mRNA moves to the nucleus and activates the expression of its target genes such as homocysteine-induced ER protein (HERP). IRE1 phosphorylation also leads to c-Jun N-terminal kinase (JNK) phosphorylation and prevention of the anti-apoptotic function of Bcl-2 (B-cell lymphoma 2) and activation of the proapoptotic protein, Bcl-2 homology 3 (BH3) (46). Similarly activated PERK is dimerised and autophosphorylated leading to the phosphorylation of eIF2α which in turn leads to translationtional attenuation of most mRNA. An exception is the mRNA for ATF4, which activates several downstream genes such as C/EBP homologous protein (CHOP). Activated ATF6 moves to the Golgi where it is cleaved, releasing its basic leucine zipper and transcriptional activation domain. This domain is transported to the nucleus to induce its target genes such as BIP.

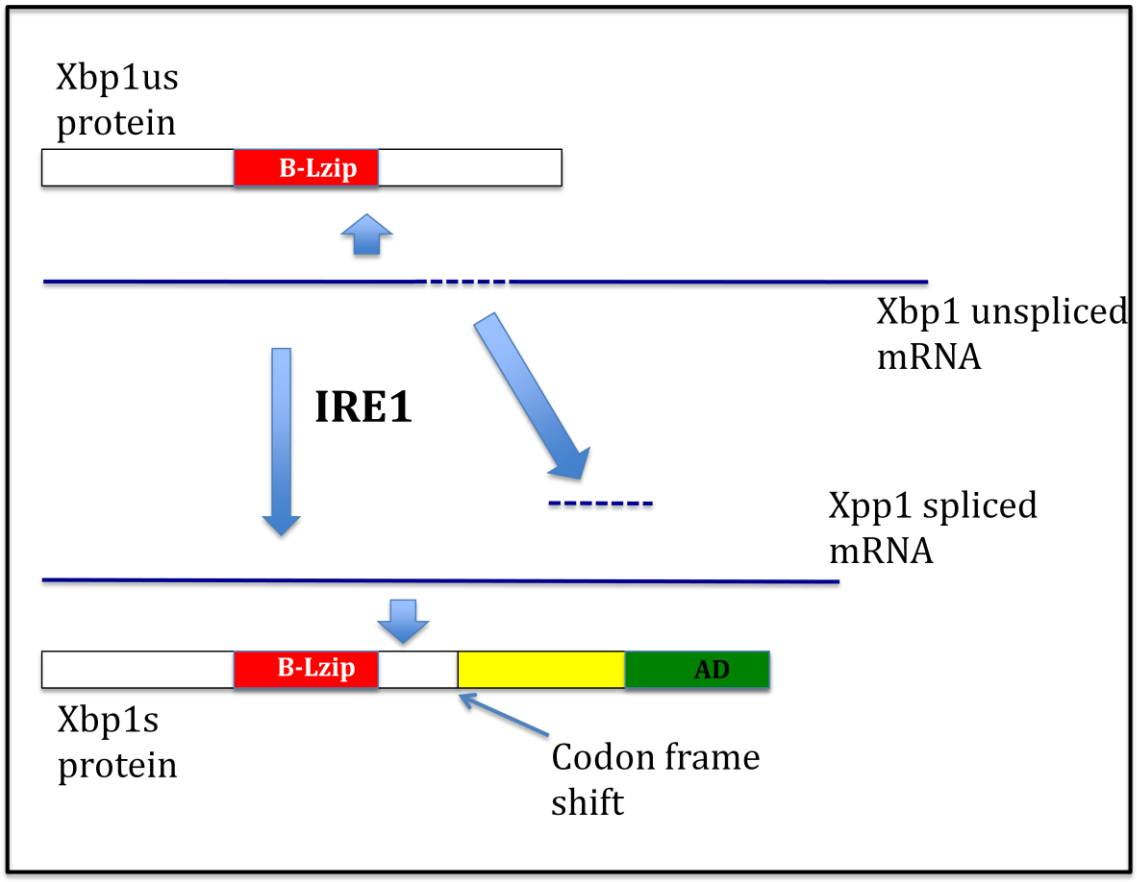

Figure 1.2. Xbp1 splicing. Unspliced mRNA for Xbp1 is translated into Xbp1 unspliced protein which has a basic leucine-zipper (B-Lzip) domain but no transcription activation domain. Activated IRE1 splices out a segment of the mRNA downstream from the coding sequences for the B-Lzip domain. This changes the codon-reading frame of the mRNA so that spliced Xbp1 mRNA codes for a protein (Xbp1s), which retains the B-Lzip domain but now also possesses a transcription activation domain (AD).

1.1.5. PERK

In ER stress, the release of BIP from PERK allows PERK dimerization and activation by auto phosphorylation. The activated dimer phosphorylates the α subunit of eukaryotic translation initiation factor 2 (eIF2α) and attenuates the protein synthesis. This prevents the activation of eIF2α by inhibiting exchange of guanosine diphosphate (GDP) for guanosine triphosphate (GTP) in the eIF2α-GDP-eIF2α complex. Since eIF2α-GTP-Met tRNA is required to bring the initiator methionyl-tRNA (Met-tRNA) to the 40s ribosome, the absence of free eIF2α inhibits the 40S and 60S ribosomal subunits from forming the 80S initiation complex for translation and consequently this event leads to reduction in the rate of translation (reviewed in 9, 23), figure 1.3.

Due to the presence of two upstream open reading frames (uORF) within the 5' untranslated region of the mRNA, translation of selective mRNAs such as ATF4 is promoted by phosphorylated eIF2α (79). The 5' proximal upstream uORF is a positive-acting element that aids ribosome scanning and re-initiation at downstream coding regions in the ATF4 mRNA. When eIF2-GTP is abundant in nonstressed cells, ribosomes scanning downstream of uORF1 reinitiate at the next coding region, uORF2, and an inhibitory element that blocks ATF4 expression. During stress conditions, phosphorylation of eIF2 and consequently reduction in the level of eIF2-GTP increases the time required for the scanning ribosomes to become competent to reinitiate translation. This delayed reinitiation allows for ribosomes to scan through the inhibitory uORF2 and instead reinitiate at the ATF4-coding region (79, 83), figure 1.4.

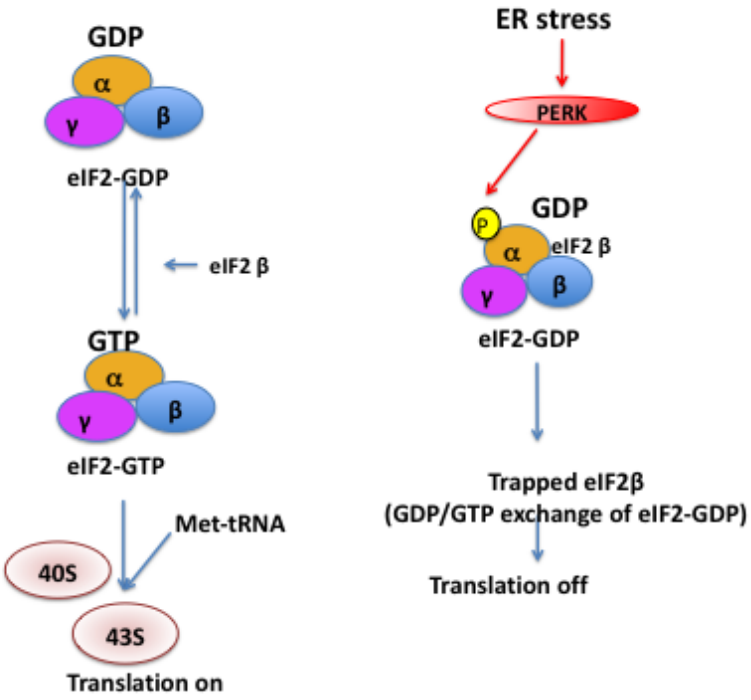

Figure 1.3. eIF2 and protein synthesis. eIF2 is composed of the three subunits α, β and γ. The GTP-bound eIF2 delivers the methionyl-charged initiator transfer RNA to the 40S ribosomal subunit as a ternary complex. At the end of initiation, the GTP on eIF2 is hydrolyzed, producing inactive eIF2-GDP. Active eIF2 is recycled by the guanine nucleotide exchange factor, eIF2β. Phosphorylation of the subunit of eIF2 leads to sequestration of eIF2β, accumulation of eIF2-GDP, and inhibition of protein synthesis by lack of delivery of the first amino acid (9, 23).

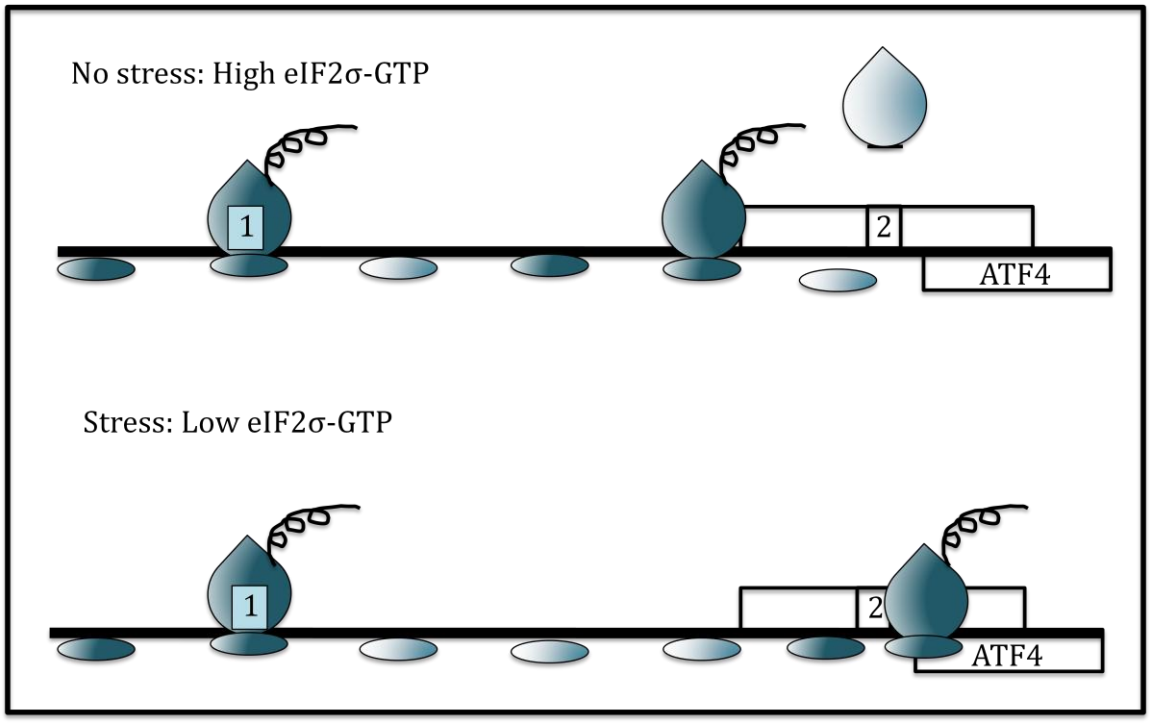

Figure 1.4. ATF4. Model for ATF4 translational control by its leader sequences. The *ATF4* mRNA is illustrated as a straight line with two upstream Open Reading Frames (uORFs) 1 and 2 in the 5' leader, which are presented as boxes. The shading of the small ribosomal subunit indicates its association with eIF2-GTP bound Met-tRNA$_i^{Met}$. The 5' proximal uORF1 is a positive-acting element that facilitates the ribosme scanning and reinitiation at downstream coding regions in the ATF4 mRNA. When eIF2-GTP is abundant in nonstressed cells, ribosomes scanning downstream of uORF1 reinitiate at the next coding region, uORF2, an inhibitory element that blocks ATF4 expression. During stress conditions, phosphorylation of eIF2 and the accompanying reduction in the levels of eIF2-GTP increase the time required for the scanning ribosomes to become competent to reinitiate translation. This delayed reinitiation allows for ribosomes to scan through the inhibitory uORF2 and instead reinitiate at the ATF4-coding region (79).

Translation of transcription factor ATF4 and its translocation into nucleus induces the expression of genes that function in amino acid metabolism, antioxidant response, and regulation of apoptosis including C/EBP homologous protein (CHOP), growth arrest and DNA damage (GADD)34 and ER oxidoreduction1 like protein (EROL1). After recovery from the UPR, GADD34 targets protein phosphatase 1 (PP1) to dephosphorylate eIF2α and increase protein translation (reviewed in 29, 38, 68).

1.1.6. Activating transcription factor 6 (ATF6)

This UPR sensor is formed by ATF6 and its homologs. In non-stressed condition BIP binds to the luminal C terminus of ATF6 and masks its two Golgi localization signals preventing ATF6 activation by regulated intramembrane proteolysis (70). There are two forms of ATF6, ATF6α (90 kDa) and ATF6β (110 kDa, also known as CREB-RP). ATF6 is synthesized as an inactive precursor that associates with ER as a transmembrane protein. The effector portion of ATF6 contains the DNA binding and transcriptional activation region, which is located at the N terminus, in the cytoplasm.

Activation of UPR leads to the transport of ATF6 to the Golgi, where regulated intramembrane proteolysis by site 1 and 2 proteases (S1P) and (S2P) releases its cytoplasmic domain containing the basic leucine zipper and activation domain (87). Activated ATF6 migrates to the nucleus and induces transcription of its target genes for ER chaperones such as Glucose Regulatory Protein 78 (GRP78), Glucose Regulatory Protein 94 (GRP94), calreticulin and ERAD components. ATF6 recognizes ER responsive elements (ERSE) in the promoters of these genes (reviewed in 3, 23, 38) figure 1.5. Transcriptional factors that are related to ATF6 include LZIP (also known as Luman or cyclic AMP-responsive element binding protein 3 (CREB3), OASIS (also known as CREB3- like1 and Tisp40 (transcript induced in spermiogenesis (reviewed in 3, 23, 67, 68).

1.1.7. Viruses and UPR

Viruses often induce host cells to produce large amount of viral proteins, many of which undergo glycosylation and other modifications in the ER, causing stress to the ER and consequently UPR activation. Some consequences of the UPR such as expression of chaperones and regulation of the metabolism may be useful to the viral replication. However, protein

synthesis attenuation and apoptosis may not be conducive to maximal viral replication. Due to the dependency of viruses on the host protein synthesis machinery, many viruses have evolved different mechanisms to selectively activate portion of the UPR that alleviate ER stress but counter the attenuation of the protein synthesis brought about by the activation of PERK.

Studies (33, 85) have shown that human cytomegalovirus (HCMV) infection induces the UPR but modifies the effects of the three UPR (PERK, ATF6 and IRE1) pathways in order to eliminate its harmful effects. Isler showed that even though HCMV significantly activated PERK during infection, it maintained translation by limiting eIF2α phosphorylation. This might be possible through an increase in the amount of total eIF2α in infected cells (24). Although eIF2α phosphorylation was limited in HCMV infected cells, translation of transcription factor ATF4, which is normally dependent on eIF2α phosphorylation, did occur. This could be explained by the fact that the translation of ATF4 occurs at very low levels of phosphorylated eIF2α (11, 12).

Expression of ATF4 activated the genes that are involved in maintaining cellular metabolism and redox, increasing chaperones and foldase capacity. An example of the genes product is Growth Arrest and DNA Damage Inducible protein (GADD34), which benefits the infection by dephosphorylating phospho eIF2α. GADD34 interacts with protein phosphatase 1 to dephosphorylate eIF2α and consequently maintain protein synthesis (4). Also it has been shown that HCMV protein pUL38 modulates the UPR through inducing ATF4 expression, inhibiting persistent JNK phosphorylation and suppressing ER stress-induced cell death (85).

Although HCMV infection inhibited ATF6 activation, it activated ATF6 target genes such as BIP & GRP94 in a gene specific manner independent of ATF6 activation (33). Activation of these genes benefits the virus by aiding in protein folding and preventing protein aggregation. HCMV also activated the IRE1 pathway, induced splicing of Xbp1 mRNA but transcriptional activation of Xbp1 target gene EDEM was not detected. This suggests that either the levels of spliced Xbp1 mRNA in HCMV infected cells were too low to produce sufficient Xbp1 protein or the transcriptional activity of Xbp1 was inhibited by the virus (33).

Hepatitis C virus (HCV) is intimately associated with ER. HCV envelope protein biogenesis, RNA replication and virus assembly occur in ER-derived membranes. In addition, the UPR induces autophagy required for viral RNA maturation and prevention of interferon-β activation through HCV derived pathogen-associated molecular pattern

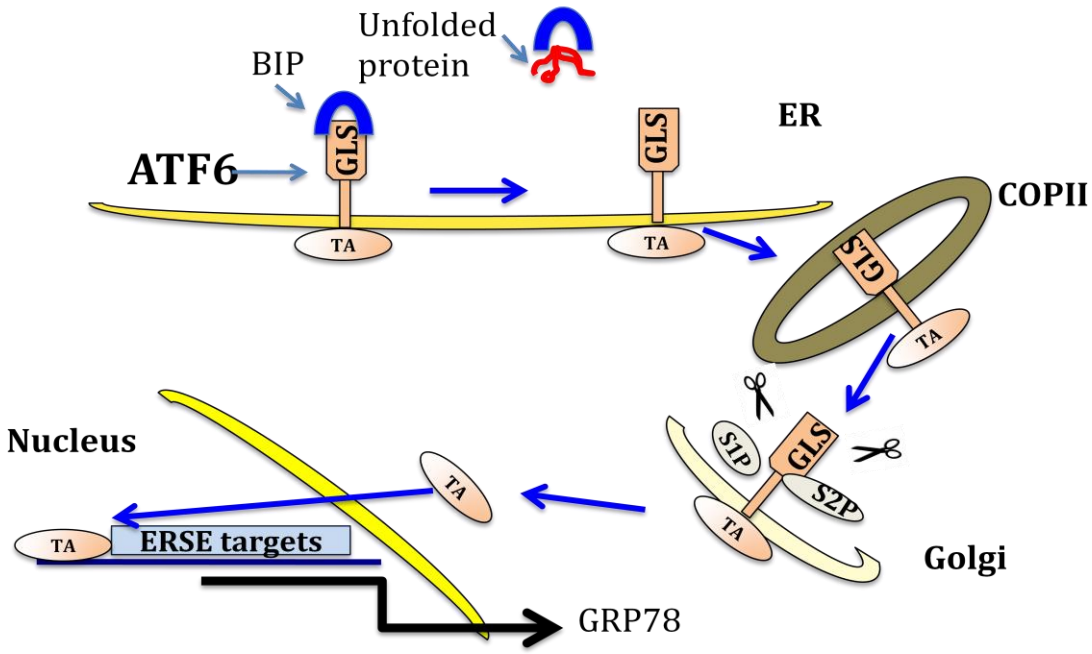

Figure 1.5. ATF6. ATF6 is held in the ER by interactions with the chaperone GRP78 (BIP). ER stress caused by accumulation of unfolded proteins in the ER, results in release of BIP, exposing a Golgi localization sequence (GLS) on ATF6 that targets it to the Golgi in COPII vesicles. There, a sequential cleavages by site 1 and 2 protease (S1P and S2P) frees the basic leucine zipper and transactivation domain (TA) of ATF6 to translocate to the nucleus, where it binds the ER stress response element (ERSE) and activates genes including GRP78 (87).

(PAMP, 38). HCV proteins activate the UPR. Expression of envelope proteins E1 and E2 leads to Xbp1 mRNA splicing and expression of transcription factor C/EBP homologous protein (CHOP)(5) and HCV non-structural protein NS4B induces Xbp1 mRNA splicing and ATF6 activation (92) by perturbing calcium homeostasis in the ER (49).

Tardif et al. (75) showed that HCV replication induced and regulated the UPR. In HCV infected cells, ATF6 was converted to its transcriptionally active form, which induced its target gene GRP78, a major target of the UPR. Another characteristic of the UPR is translational inhibition. However, cells with HCV replicon showed higher viral protein synthesis and lower level of eIF2α phosphorylation, which is evidence of increased translation initiation.

In addition, Pavio et al. (63) illustrated that the HCV envelope protein E2 aids virus to escape the negative translational effects of ER stress. Although E2 protein at low expression level induced ER stress, at high expression levels, and *in vitro*, it bound and inhibited PERK kinase activity, preventing eIF2α phosphorylation, thus allowing translation to proceed.

In contrast to many viruses, Coxsackievirus B3 (CVB3) takes advantage of the apoptotic aspect of UPR activation in order to release viral progeny (6, 71). CVB3 infection activates all three arms of the UPR and induces apoptosis through the downregulation of p58 and induction/activation of two stress induced transcription factors; C/EBP homology protein (CHOP), and Sterol Regulatory Element-Binding Protein (SREBP1) (91).

In addition, hepatitis B virus regulatory x protein (HBx) has been demonstrated to be an inducer of UPR and the activator of the ATF6 and IRE1-Xbp1 pathways. In Hep3B cells with transient or stable expression of HBx, GRP78, spliced Xbp1 and cleaved ATF6 proteins were detected, suggesting that the ATF6 and IRE1-XBP1 pathways were activated (47).

The study done by Faveau et al. demonstrated the role of the human coronavirus OC43 S glycoprotein in differential induction of the UPR and consequently in the viral neuroinvasive properties. They used coronavirus OC43 variant harboring a persistence-associated mutation in the S glycoprotein and showed that the mutant virus induced stronger UPR activation and translation attenuation in infected human neurons, comparing with the wild type virus. Although both mutant and wild type viruses activated the IRE1 / Xbp1 pathway, they did not activate ATF6 and ATF4 pathways (15).

Arenaviruses also have been shown to selectively induce the UPR. Acute infection with lymphocytic choriomeningitis virus (LCMV) a member of Arenaviruses resulted in activation of ATF6 pathway and upregulation of its target genes such as BIP, GRP78 and GADD34 whereas PERK and IRE1 pathway were neither activated nor blocked. LCMV infection not only activated the ATF6 pathway but it also affected the sensitivity of ATF6 regulated branch of UPR to further stress such as thapsigargin treatment. The Viral glycoprotein precursor protein (GPC) is responsible for activating the ATF6 branch of UPR in LCMV infection (62).

Ambrose et al. (1) showed that West Nile virus strain Kunjin (WNV $_{KUN}$) differentially induced ATF6 and IRE1 activation and this activation of UPR coincided with the peak of viral RNA and protein production. While IRE1 and ATF6 activation resulted in high level of Xbp1 splicing and BIP transcription, no activation in PERK/eIF2α was observed. WNV $_{KUN}$ hydrophobic nonstructural proteins NS4A and NS4B have been identified as the potent inducers of UPR (1)

1.1.8. HSV and UPR

During the HSV-1 productive phase, viral protein synthesis may overload the ER's folding capacity and induce UPR. However, HSV-1 has evolved different strategies to counter the protein synthesis attenuation aspect of the UPR. Although HSV-1 induces PERK activation, the viral protein $\gamma_1$34.5 activates growth arrest and DNA damage gene 34 (GADD34) that targets and interacts with phosphatase to dephosphorylate eIF2α to enable continued protein synthesis (7, 26, 60).

Mulvey et al., have shown that not only do PERK and IRE1 remain inactive in HSV-1 infected cells, PERK selectively resists activation by ER stress. In infected cells, HSV glycoprotein B (gB) specifically binds to the luminal domain of PERK and inhibits the activation of its kinase (60). By selectively preventing PERK activation, HSV-1 gains the additional advantage of not inducing the synthesis of CHOP (PERK target gene) and its subsequent induction of apoptosis, which may be detrimental for virus life cycle (94).

1.2. Herpes simplex Virus-1 (HSV-1)

1.2.1. The *Herpesviridae* family

Herpesviridae is a family of large, icosahedral, enveloped, double-stranded DNA viruses that replicate in nucleus of their host cells. Members of *Herpesviridae* can infect a wide variety of vertebrate hosts. This family is characterized by the unique pattern of gene expression and their ability to establish life long latent infection. Eight herpesviruses out of more than 200 that have been identified in nature have humans as their primary host: herpes simplex virus 1 (HSV-1), herpes simplex virus 2 (HSV-2), human cytomegalovirus (HCMV), varicella-zoster virus (VZV) and Epstein-Barr virus (EBV), and Human herpesviruses 6, 7, and 8 (HHV-6, HHV-7, and HHV-8, (reviewed in 66).

The *Herpesviridae* family is subdivided into subfamilies *Alphaherpesvirinae, Betaherpesvirinae,* and *Gammaherpesvirinae* based on biological properties, DNA sequence similarity, host range, growth rate and cell types in which they establish latency (66).

Alphaherpesvirinae includes herpes simplex virus (HSV- 1 & 2), which cause oral and genital herpetic lesions and varicella-zoster virus (VZV), the cause of chickenpox and shingles. The members of this subfamily have a variable host range, relatively rapid and destructive reproductive cycle and establish latent infection in sensory neurons.

Betaherpesvirinae includes human cytomegalovirus (HCMV), and Human herpesviruses 6, 7, and 8 (HHV-6, HHV-7, and HHV-8). They generally grow slowly and lead the infected cells to become enlarged (cytomegalia), establish latency in kidney, lymphoreticular cells and secretory glands cells.

Finally the subfamily *Gammaherpesvirinae* contains Lymphocryptovirus Epstein Bar virus (EBV) and Rhadinovirus human herpes virus (HHV-8) which often infect and establish latency in lymphoid cells (reviewed in 66).

1.2.2. HSV-1 lytic and latent infection

The life cycle of HSV involves both lytic (productive) and latent (non-productive) phases. The initial lytic phase of HSV-1 virus begins with the first exposure of host epithelial cells to HSV-1, followed by viral replication in these cells and in the sensory neurons innervating the skin. In the lytic phase, virus replication stimulates the host response causing a lesion (cold sore),

which heals in a few days. The symptoms of lytic phase disappear, but infection persists in a latent state in sensory neurons. Periodic reactivations can occur when the host is affected by a variety of stimuli such as fever, sunburn, inflammation and physiological or psychological stresses. Following reactivation, the virus replicates in the neurons and travels back along the axons to the original site of virus entry and infection causing a productive lesion and clinical symptoms (reviewed in 66).

1.2.3. HSV virus structure

The HSV virion is an average of 186 nm to 225 nm diameter including spikes. It consists of four parts: (a) core containing the viral DNA, (b) icosahedral capsid surrounding the core, (C) the unstructured proteinaceous layer between the capsid and the envelope called the tegument, and (d) an outer lipid bilayer envelope with spikes on its surface (reviewed in 66).

1.2.3.1. Core

The core contains the double strand DNA genome composed of 153 kilo base pairs with a G+C content of 68% for HSV-1 and 69% for HSV-2 (40).

1.2.3.2. Tegument

The tegument is an unstructured protein matrix located between the envelope and the capsid. It is composing of at least 20 viral proteins such as host shut-off protein (VHS) with the capacity to degrade the cellular and viral mRNA, VP22 which plays a role in spreading the virus from cell to cell and the virion transactivator factor, VP16 (reviewed in 66) .

1.2.3.3. Capsid

The capsid is composed of 162 capsomers arranged in a T=16 icosahedral symmetry. The outer shell of capsid consists of four viral proteins, VP5, VP26, VP23 and VP19. VP5, the major capsid protein, present in both penton and hexon capsomers. VP26 is present in hexon. One VP19 molecule and two VP23 molecules make up the triplexes that link adjacent capsomers (93). The capsid also contains VP24, the protease and UL16 which are involved in DNA encapsidation (reviewed in 66).

1.2.3.4. Envelope

The envelope of HSV is derived from a host cytoplasmic membrane. It contains a lipid bilayer with eleven transmembrane viral proteins embedded in it, such as glycoproteins gB, gC,

gD, gE, gG, gI, gH, gL, gM and two nonglycosylated intrinsic membrane proteins Us9 and U_L20 (reviewed in 66).

1.2.4. Viral genes regulation during lytic infection

1.2.4.1. IE, E, L genes

During lytic infection, more than 80 HSV genes are expressed in a highly regulated cascade. Immediate early (IE) genes are expressed very soon after infection. The six proteins are designated ICP0, ICP4, ICP22, ICP27, ICP47, and US1. ICP0 and ICP4 are transcriptional activators. ICP0 activates transcription of both viral and cellular genes. The next set of HSV genes to be expressed, are called early genes (E). They are expressed approximately 4 to 8 hours post infection and for their expression they require the presence of functional ICP4 protein. Early genes code for proteins that are required for viral replication, include thymidine kinase (tk) and DNA polymerase. Late genes (L) include genes coding for US11, gC (UL44), gB (UL27), VP16 and VHS. They are the last genes to be expressed. Their expression reaches peak levels after viral DNA synthesis has started (reviewed in 66).

1.2.4.2. Initiation of the lytic cycle by VP16, Host Cell Factor and Oct-1

IE genes transcription is initiated by the assembly of a multi-protein complex consist of virion protein 16 (VP16) and two cellular proteins: Oct-1 and Host Cell Factor (HCF). Oct-1 is a transcription factor belonging to the Pit-Oct-Unc (POU) family (27). HCF is a chromatin-associated protein that may be involved in many cellular functions such as cell cycle progression. It was initially discovered through its role as a co-factor required by VP16 to initiate HSV IE genes expression (42). VP16 is an essential structural component of the virus that is synthesized at the L phase of HSV lytic infection and then integrated into the virus tegument. Following lytic infection, VP16 is released into the cell and associates with HCF. HCF promotes the nuclear translocation of VP16 (44) and is also a co-activator of VP16 (54). VP16/HCF heterodimer recognizes the POU domain of Oct-1 bound to TAATGARAT (where R is a purine) motifs present in multiple copies in the promoters of all HSV IE genes and induce their transcription and finally their expression. Viral IE proteins later regulate the expression of E and L genes (reviewed in 66). For active IE genes transcription, VP16 recruits histone acetyltransferases and remodeling enzymes to remove histone from the promoters of these genes (28, 80).

1.2.5. Latent infection

1.2.5.1. Latency establishment and maintenance

HSV-1 infects the ends of sensory neurons innervating the epithelial site of primary infection. The capsid is transported to the nucleus of the sensory neurons (trigeminal ganglion in HSV-1) where it undergoes the lytic cycle and the death of the infected neurons or it establishes a latent infection in about 3% of the neurons (reviewed in 66).

In contrast to lytic infection where the viral genome retains a linear conformation, during latency the HSV genome is circular and assembled into a nucleosomal structure. Most of evidences suggest that in contrast to the lytic phase, during latency, expression of all lytic genes are silenced and the only viral gene expression detected is LAT (reviewed in 65, 66). LAT promoter is insulated from hyperacetylated lytic cycle genes (2).

While no protein expression has been associated with LAT, observations show that it contributes to latency in many ways. One potential role of LAT is to prevent infected neurons from committing apoptosis. Prevention of apoptosis has been related to two regions of transcript that are capable of interfering with the caspase-9 pathway (35, 39). In addition, transfection of a plasmid expressing LAT protects cells from caspase 3 induced apoptosis (34, 48).

Recently, Kather et al. have shown that HSV-1 antiapoptotic LAT is associated with the downregulation of cellular FLICE (FADD-like IL-1β-converting enzyme)-inhibitory protein (c-FLIP) a potent inhibitor of caspase-8-mediated apoptosis (36).

It is believed that LAT enhances latency by repression of the viral IE genes such as ICP0, ICP4 and ICP27 (13, 41). Infection of neuronal cell clones that stably express LAT results in great reduction in the level of IE genes transcripts (19, 64). Recent studies have implicated micro RNAs (miRNAs) in this phenomenon (74, 77). This is thought to be through silencing of the IE genes. The last 750 bases of LAT are complementary to ICP0 gene (14).

LAT encodes a function that increases the amount of dimethyl lysine 9 form of histone H3 or heterochromatin and reduces the amount of dimethyl lysine 4 form of histone H3, a part of active chromatin, on viral lytic-gene promoters. Thus LAT may manipulate the cellular histone modification machinery to repress its lytic-gene expression, thus converting portions of viral DNA into a non-productive form known as heterochromatin (80).

Several studies support the idea that latency is the consequence of failed initiation of IE genes expression. This may be the result of the virus failure to assemble the VP16-HCF-Oct-1 complex, which is required for activation of IE genes promoters. Some explanations for this include: absence or inability of VP16 to reach neuronal nucleus during the axonal transport (43, 65), low level of Oct-1 (78), cytoplasmic sequestering of HCF in sensory neurons (43) and the presence of other POU family in sensory neurons, such as Oct-2 that can compete with Oct-1 for binding to TAATGARAT sequence in the IE genes promoters (50, 51).

There is also immunological evidence that structural proteins are expressed at intermittent low-levels in some latently infected neurons and stimulate the immune system to prevent reactivation (10).

1.2.5.2. HSV-1 reactivation from latency

Reactivation of latent HSV in human occurs following physical trauma, physical or emotional stress, exposure to UV light, hypothermia and hormonal imbalances (reviewed in 66). While the conditions surrounding the causes of reactivation and the responsible stimuli have been studied thoroughly, the molecular mechanisms underlying HSV-1 reactivation from latency are poorly defined. During reactivation infectious virions are produced in a small number (0.05%) of latently infected neurons, which transport virus back to the site of primary infection through innervating axons. Although the neurons that become involved in lytic viral replication do not survive, the large reservoir of latently infected neurons allows this cycle to occur repeatedly (58).

While during lytic infection in tissue culture cells, temporal pattern of IE, E and L genes expression has been well described, the pattern of viral gene expression during reactivation in neuronal cells has not been characterized.

At present, it is believed that the VP16 transactivating function is not required for the exit from latency. Therefore, one critical question is raised: How does the latent viral genome initiate the transcription of IE genes in the absence of VP16?

The observation made by Tal-Singer et al. suggests that the viral gene expression may be regulated differently during reactivation (73). Early viral transcripts were detected before immediate-early transcripts. This means cellular stimulus causing reactivation does not act specifically on the IE class of viral genes but rather acts on a broader class of viral genes (73).

Another recent study emphasizes on the role of VP16 in both the lytic infection and reactivation (76). The authors argue that in neurons, VP16 is expressed with different kinetics

than in non-neuronal cell types. They present a model whereby de novo synthesis of VP16 is required to induce reactivation within the neurons. Following stress, the VP16 promoter is activated in latently infected neurons in the absence of other viral proteins.

Cellular stresses result in changes to the neuronal transcription pattern which exclusively affect the VP16 promoter, allowing the expression of VP16 protein in reactivated neurons. Once enough VP16 is produced, IE gene expression can be stimulated by produced VP16 and temporal cascade of genes expression initiated (56).

1.2.5.3. Neuronal model of HSV-1 infection

Although animals such as mice and rabbits have been used as *in vivo* models for HSV-1 studies for a long time, cell culture models provide the ability to easily manipulate infected cells and observe the virus without the host immunological interactions. Cell cultures are very useful for studying the molecular details of HSV-1 life cycle in different lytic and latency phases. Primary neuronal cell cultures of neonatal rat dorsal root ganglia (DRG) and neuronal cell lines such as rat pheochromocytoma (PC12) (8), human neuroblastoma (IMR32) (90) are used to study HSV-1 neuronal cell interactions .

A very useful *in vitro* cell model is PC12, which differentiates into cells with similar sympathetic neurons. Even though PC12 cells have been used extensively in HSV studies specially for NGF treatment (22), their disadvantage is that they are rat cells and are not human neurons. To have a better understanding of HSV-1 infection in a similar condition to *in vivo* human HSV infection, in my project, I used human neurons, ONS- 76 cells as a model for neuronal cells for HSV-1 infection. This cell line has been derived from human medulloblastoma cells a highly malignant primary brain tumor that originates in the cerebellum or posterior fossa (86).

1.3. Hypothesis

I hypothesize that HSV-1 infection in epithelial and neuronal cells modulates the UPR in a selective manner so that functions of UPR that are beneficial for viral replication are activated while those that may suppress replication are not.

1.3.1 Main objective

To test the hypothesis that during HSV-1 infection in epithelial (Vero) and neuronal (ONS-76) cells the Unfolded Protein Response (UPR) is selectively activated.

1.3.2. Specific objectives:

1.3.2.1. To establish the time course of various parameters of viral replication in Vero (epithelial) and ONS-76 (neuronal) cells.

a) Time course of infectious virus production
b) Time course of viral DNA replication
c) Time course of transcription of representative viral Immediate Early (IE), Early (E), and Late (L) genes
d) Time course of synthesis of representative IE, E, and L proteins
e) To determine if the expression of VP16 (L protein) requires the expression of new protein synthesis in ONS-76 cells

1.3.2.2. To evaluate the efficiency of the primers designed to quantify the transcription of genes representative the three arms of UPR (IRE1, PERK, ATF6)

To monitor Xbp1 (spliced), homocysteine-induced ER protein (HERP)(29), CHOP (91) and GRP78/BIP (88) transcripts in Vero and ONS-76 cells treated with thapsigargin

1.3.2.3. To determine if expression of the genes representing of the three main pathways of UPR are affected during infection with HSV-1

a) To monitor Xbp1 (spliced), HERP, CHOP and GRP78/BIP transcripts in Vero and ONS-76 cells infected with HSV-1
b) To examine the level of eIF2α phosphorylation protein in infected cells by Western blot

1.3.2.4. To study if HSV-1 can selectively inactivate components of the UPR

To examine the effect of HSV-1 infection on activated UPR in Vero and ONS-76 cells

1.3.2.5. To determine if ICP0 or VP16 viral genes are required to shut off the UPR

The goal of the this study was to find out whether and how HSV-1 regulates the UPR during viral infection to prevent the UPR detrimental affects and promote its protein synthesis.

By correlating differences in the various parameters of viral replication with components of the UPR in permissive (Vero) and semi permissive (ONS-76) cell I hope to identify the viral factors that contribute to the UPR regulation.

CHAPTER 2: Material and methods

2.1. Cell culture

All chemicals and media were ordered from Invitrogen (Carlsbad, CA, U.S.A.) unless otherwise stated. Cells were grown in monolayers in 75 cm^2 tissue culture flasks. African green monkey kidney (Vero) cells were maintained in Dulbecco's modified Eagle's medium (D-MEM) with 10% newborn calf serum and 100 units of penicillin- streptomycin per ml. The human medulloblastoma cell line, ONS-76 was obtained from Michael Taylor (University of Toronto, Canada) and grown in D-MEM medium with 10% fetal bovine serum (FBS) and 100 units of penicillin-streptomycin per ml. For all experiments, cells were plated at a density of 2 X 10^5 cells per well in 6 well culture plates (BD Falcon, Mississauga, ON, Canada) and incubated in a 5% CO_2 humidified atmosphere at 37°C. Cells were plated 24 h prior to viral infection, transfection or other treatments.

2.2. Virus

For HSV-1 infection, strain KOS was used. HSV-1 KOS viral stocks were prepared in Vero cells and virus titers determined by standard plaque assay on Vero cell monolayers. Infections were carried out at a multiplicity of infection (MOI) of 5 plaque forming units (pfu) per cell in D-MEM without serum. After incubation for 1 hour, with gentle rocking every 15 minutes, the inoculum was replaced with D-MEM plus 5% serum and the cells were maintained at 37°C for indicated times. Mock infection was carried out by adding media without viral inoculum to the cells.

2.3. Single-Step Growth Curve

Single step growth (21) experiments were performed to determine the virus growth rate in Vero and ONS-76 cells. Both Vero and ONS-76 cells were plated at 2 X 10^5 cells per well in 6 well plates. After 24 hours the cells were infected with HSV-1 at a MOI of 5 pfu per cell. After one-hour incubation, the cells were washed once with phosphate –buffered saline (PBS) and then twice with low pH glycine buffer (18) to inactivate or remove any virus that had not penetrated.

Then the cells were scraped into the medium at 1, 4, 8 and 12 hours post infection and subjected to three freeze-thaw cycles. Virus titer in each time point was determined by plaque assay on Vero cells.

2.4. Plaque assay

The quantification of infectious viral particles was achieved by a standard plaque assay. Serial dilutions of virus were added to Vero cells in six well plates. After a 1 hour adsorption period, the inoculum was replaced with the mixture of complete medium containing serum and 2% low melt agarose, and incubated for an additional 2 days. The plates were then stained with media containing 0.5% neutral red and the numbers of plaques were counted after 24 hours. Titers were calculated as PFU per ml of virus suspension.

2.5. DNA purification and analysis

To determine the number of viral genomes per unit mass, the following calculations were made based on the facts that the number of base pair (bp) in one genome of HSV-1 is 1.5×10^5 and a base pair of double-strand DNA has a molecular mass of 650. Therefore, molecular weight (1 mole) of HSV-1 genome was calculated by multiplying 650 to 1.5×10^5, which is equal to 975×10^5 gram. The number of molecules of HSV-1 per gram was calculated by dividing 6.02×10^{23} by 975×10^5, which is equal to 6×10^{15} molecules of the HSV genome per gram. qRT PCR was performed on serial dilutions of HSV-1 DNA by using primers flanking a 327 bp segment of the HSV-1 thymidine kinase (TK) gene. Genome equivalents and its log 10 for each diluted HSV-1 DNA were calculated. Using the log genome equivalents vs Ct values a standard curve was generated. To calculate the DNA concentration in each sample, the Ct value of the sample was used in the equation of the standard curve. Finally the genome equivalent for each sample was calculated by taking the antilog of the DNA concentration.

2.6. RNA purification and Real time PCR (qRT PCR) analysis

Total RNA was extracted from cells in 6 well cell culture plate using RNeasy plus mini kit (Qiagen) as suggested by manufacturer. Quantification of RNA was performed using Thermo

Scientific Nanodrop 2000C. Two μg of total RNA was used for cDNA synthesis using Quantitect Reverse transcription kit (Qiagen). To detect and quantitate transcripts, Briliant II SYBER Green QPCR Master Mix (Agilent technology, Mississauga) was used. Samples were amplified in an Mx 3005P QPCR thermocycler (Stratagene). The thermocycling condition consisted of initial activation step for 10 minutes, 40 cycles of amplification using a plateau of 95°C/30 seconds for denaturation, followed by a plateau of 55°C/1 minute for annealing, and a plateau of 72°C/30 seconds for extension. Amplification data were collected at the end of each annealing plateau. Segment 3 contains the dissociation curve. The default profile dissociation curve begins with a 1-minute incubation at 95°C to melt the DNA and then a 30-second incubation at 55°C.

Gene expression levels relative to house keeping gene GAPDH were determined according to the $2^{-\Delta\Delta CT}$ method (52) as follow: ΔCt values calculated by deducting the GAPDH Ct value from the Ct value of test sample , ΔΔCt value calculated by deducting of ΔCt value of test samples from ΔCt value of control. Fold change was determined by calculating the $2^{-\Delta\Delta CT}$ for each sample. Since uninfected cells have no viral RNA their Ct values in qRT PCR are read about 34 Ct. For the comparison purpose, results then were calculated based on the maximum percentage; the highest level of fold change for each transcript was considered as a 100 percent and the fold change for the rest of time points were multiplied to 100 and divided to this maximum level of fold change. All primer sets for transcript amplification were purchased from Integrated DNA technologies (Coralville, Iowa, U.S.A.) except TK (Sigma-Aldrich, Oakville, On, Canada). Primers were used at 1.9 μM concentration. The sequences of the primers were as it seen in table 1.

Primer name	Direction	Sequence
ICP0	R	5’-TTGTTCAGGTAAGGCGACAG-3’
	F	5’-CTCCTCTGCCTCTTCCTCCT-3’
VP16	R	5’-AGGGCATCGGTAAACATCTG-3’
	F	5’-GGACGAGCTCCACTTAGACG-3’
TK	R	5’-CCAGTAAGTCATCGGCTCGG-3’
	F	5’-CCATCAACACGCGTCTGCGTT-3’
VP5	R	5’-CCACTTTCAGGAAGGACTGC-3’
	F	5’-CTTCTGCGAGACGAGCTTTT-3’
GAPDH	R	5’-GGGCCATCCACAGTCTTCTGGG3’
	F	5’TGCCTCCTGCACCACCAACTGC-3’
Xbp1 (spliced) without intron	R	5’-TAAGGAACTGGGTCCTTCTGG-3’
	F	5’-TCTGCTGAGTCCGCAGCAGG-3’
HERP	R	5’-CTTTGGAAGCAAGTCCTTGA-3’
	F	5’-CCGAGCCTGAGCCCGTCACG-3’
CHOP	R	5’-TGCCACTTTCCTCTCGTTCT-3’
	F	5’-TGGAAGCCTGGTATGAGGAC-3’
BIP	R	5’-GGTAGAACGGAACAGGTCCA-3’
	F	5’-GGCTTGGATAAGAGGGAAGG-3’

Table 2.1. List of primers and their sequences

2.7. Western blot analysis

At different time points post HSV-1 infection, as specified in the figure legends, the medium was completely removed from the cell monolayers. The cells were lysed and harvested with 150 μl sample buffer. Samples were boiled for 3 minutes and sonicated for 3 seconds. Proteins in cell lysates were separated by sodium dodecyl sulfate-polyacrylamide gel electrophoresis (SDS-PAGE). Proteins were transferred to Amersham Hybond-LFP membrane (GE. Healthcare, Baied'Urfe, QC, Canada) which were blocked either with 5% bovine serum albumin or 5% nonfat milk (for phospho eIF2α) and then incubated for 1 hour with primary monoclonal antibody against VP16 (LP1) obtained from Peter O'Hare, (Marie Curie Research Institute, Surrey, United Kingdom), ICP0 (mouse monoclonal antibody Santa Cruz biotechnology, Santa Cruz, CA. U.S.A.)), TK (goat polyclonal antibody, Santa Cruz biotechnology), VP5 (mouse monoclonal antibody, Santa Cruz biotechnology), GAPDH (mouse monoclonal antibody, Chemicon, Billerica, MA, U.S.A.), eIF2α (mouse monoclonal antibody, Santa Cruz biotechnology) and phospho eIF2α (rabbit monoclonal antibody, Cell Signaling technology, Pickering, ON, Canada). The membranes were then rinsed in either phosphate-buffered saline (PBS) or Tris buffered saline (TBS) for phospho eIF2α and incubated with either mouse Alexa 448 (Invitrogen), or rabbit CY5 (GE Health care). All membranes were scanned by Typhoon 3 laser fluorescence and chemiluminescence scanner with ImageQuant software.

2.8. Cell Viability

Cell viability was assessed with the trypan blue exclusion method. Vero and ONS cells were seeded at density of 2 x 10^5 per well in six well plates. After 24 hours cells were treated for 4 hours either with 1µl DMSO (control) or 100 nM thapsigargin and then harvested using trypsin EDTA. Cells were centrifuged and resuspended in media. Cell suspension was mixed with 0.4% trypan blue dye and then visually examined and counted to determine whether cells took up or excluded dye.

2.9. Plasmids

The expression vector pRG50 that encodes VP16 was provided by Peter O'Hare (Marie Curie Research Institute, Surrey, United Kingdom), plasmid CI-110, which encodes ICP0, was a gift from Roger Everett (MRC Virology Unit, University of Glasgow ,United Kingdom) and pcDNA3 was purchased from Invitrogen. One day prior to transfection, 2x 10^5 per well of Vero cells were seeded into each of 6 well plate. Transfections were performed using Lipofectamine 2000 (Invitrogen), according to the manufacturer's instruction. Cells were transfected with the mixture of 8µl of Lipofectamin in 250µ Opti-MEM (Invitrogen) and 500ng DNA (plasmid expressing either VP16, ICP0 or pcDNA) in 250µl Opti-MEM (total volume of 500µl per well).

Next day the medium was replaced with fresh media. Forty eight hours after transfection, the cells were treated with either 100nM thapsigargin (Sigma) (ER stressor) or DMSO (solvent control) for 4 hours and harvested with lysing buffer of RNeasy plus mini kit.

2.10. Immunofluorescence

To determine the transfection efficiency, the cells transfected with plasmids pRG50, CI-110 or pcDNA3 were examined by immunofluorescent staining. Vero cells were grown on circular 18-mm diameter micro coverslips in six well plates one day prior to transfection. At 48 hours after transfection, the coverslips were rinsed once with PBS and then fixed with cold methanol. The cells incubated for 20 minutes at room temperature in blocking solution (PBS +

10% NCS), washed with PBS and incubated with either primary mouse VP16 or ICP0 antibody at dilution of 1:200 and the cell nuclei were stained with promidium iodide (Sigma). Finally, the coverslips were incubated with secondary antibody conjugated to fluorochrome mouse Alexa 488 (Invitrogen) antibody for 20 minutes and then washed with PBS. The coverslips were quickly mounted onto glass slides and subsequently analyzed with Zeiss Axiovert microscope fitted with UV optics and CCD camera. Images were captured and analyzed using Northern Eclipse software (Mississagua, Ontario, Canada).

Chapter 3: Results

3.1. Kinetics of various parameters of HSV-1 viral infection in Vero and ONS-76 cells

In this study, Vero and ONS cells were chosen for the following reasons. First, these cells provide examples of permissive epithelial cells (Vero) and human neuronal cells (ONS-76) for HSV-1 infection. Second, HSV-1 leads to lytic infection in epithelial cells whereas in some neuronal cells it can establish latency. The sequence of HSV-1 gene expression in epithelial cells has been well determined. However no published studies have described the pattern of HSV genes expression in cells of human neuronal origin. Since in subsequent experiments I examined the UPR in these two cell types to have a better idea about the events following HSV-1 infection and to study the similarities and differences in the pattern of genes expression in these cells, I established a time course of different parameters of viral infection such as virus growth rate, viral DNA replication, viral IE, E and L transcription and protein synthesis in both Vero and ONS-76 cells. These cells were infected with HSV-1 and the time course of these events was monitored.

3.1.1 Kinetics of DNA synthesis and infectious virus multiplication in Vero and ONS-76 cells

The viral DNA content of infected cells is depicted in Figure 3.1.1. a and figure 3.1.1. b. Between 7 to 9 hours post infection, viral DNA concentrations were increased in both cell lines. The viral DNA content in Vero cells increased gradually and reached maximum of 3.5 $x10^6$ genome equivalents per culture at 24h post infection. Nine hours after infection, ONS-76 cells contained $1.5x10^6$ genome equivalents of viral DNA per culture. The DNA content of these cells subsequently dropped to almost $3x10^5$ genome equivalents per culture.

The amount of infectious HSV-1 produced by Vero and ONS-76 cells is shown in Figure 3.1.1 c. Infectious virus could not be detected in either Vero or ONS-76 cells in the first 4h after infection, but after 4h the rate of infectious virions increased and in Vero cells it reached to $3.2x10^7$ pfu per culture at 12h. In contrast, the rate at which infectious virus increased was more modest in ONS-76 cells with $2.8x10^6$ pfu per culture at 12 h.

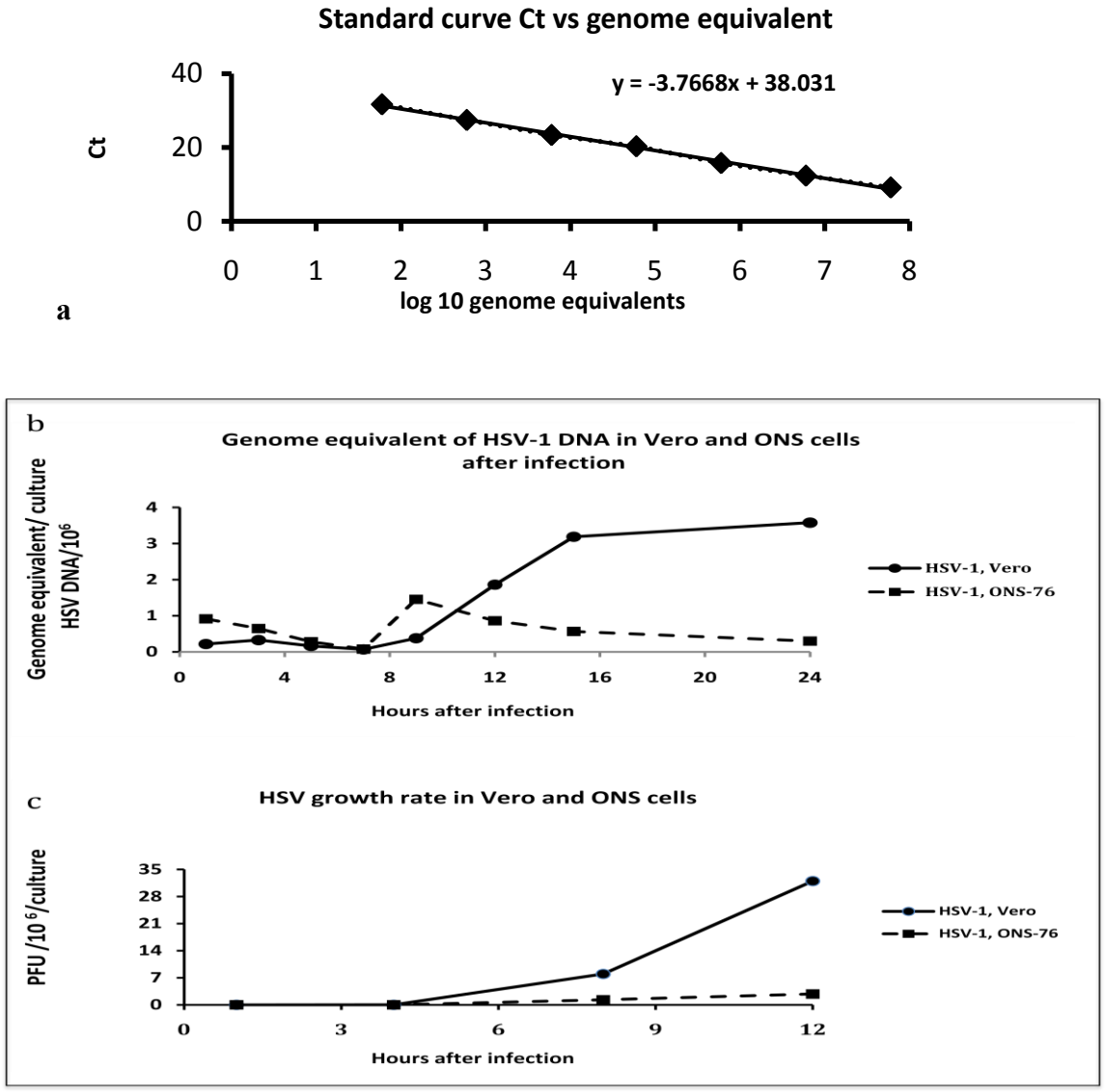

Figure 3.1.1. Time course of DNA synthesis and infectious virus production in HSV-1 infected Vero and ONS-76 cells. (a) A standard curve was created using log genome equivalents of log ten ('x' axis) vs Ct values of serially diluted HSV-1 DNA, ('y' axis) (Described in Material and Method Section). (b) Vero and ONS-76 cells were cultured at density of 2 X 10^5 per well. After 24 hours the cells were infected with HSV-1 at a MOI of 5 pfu/cell and harvested for DNA. DNA was purified from samples and qRT PCR with primers designed to amplify the TK gene were used for analyzing their viral DNA content. Ct values were used in the equation of the HSV-1 DNA standard curve (Material and Method). (c) A Single step growth experiment was performed to measure the infectious virus content in Vero and ONS-76 cells over 12 h after infection. Vero and ONS-76 cells were infected with HSV-1 virus at a MOI of 5 pfu per cell. Cells were scraped into the medium at 1, 4, 8 and 12 hours after infection and subjected to three freeze-thaw cycles. Virus titer at each time point was determined by plaque assay on Vero cells. On 'y' axis is PFU/10^6 virus per culture and on 'x' axis is the number of hours after infection. Data labels on each time point are in pfu/10^6 of virus per culture.

3.1.2. Kinetics of viral RNA expression in HSV-1 infected ONS-76 and Vero cells

The HSV-1 ICP0, TK, VP16 and VP5 genes were chosen as representatives for the IE, E and L classes of viral genes for monitoring the viral genes expression over 24 hours. Vero and ONS-76 cells were infected with HSV-1 at a MOI of 5 pfu per cell. Cells were harvested at 1, 3, 5, 7, 9, 12, 15 and 24 hours post infection and the relative transcripts expression levels for each of the various HSV-1 genes were measured by qRT-PCR. Since the level of the RNA for these genes in the two cell-types were different, the results are expressed (Fig 3.1.2) as a percentage of the maximum increase for each cell line.

As seen in the figure 3.1.2, the kinetics of ICP0 (IE) expression in both cells were similar. ICP0 RNA started to increase at about 4 hours post infection and reached maximum levels (100%) at 9 hours post infection. In contrast, the kinetics of accumulation of RNA for TK, VP16 and VP5 were different in the two cell types (figure 3.1.2). While in ONS-76 cells, the expression of these transcripts reached to a maximum at 9 and 7 hours post infection, in Vero cells the transcripts reached a maximum at 24 hours post infection. Although VP16 is considered as an L gene and its maximum expression is expected to be detected in the later hours of infection, surprisingly in ONS-76, VP16 expression reached a maximum level at 7 hours post infection. This was similar to the kinetics for ICP0, an IE gene.

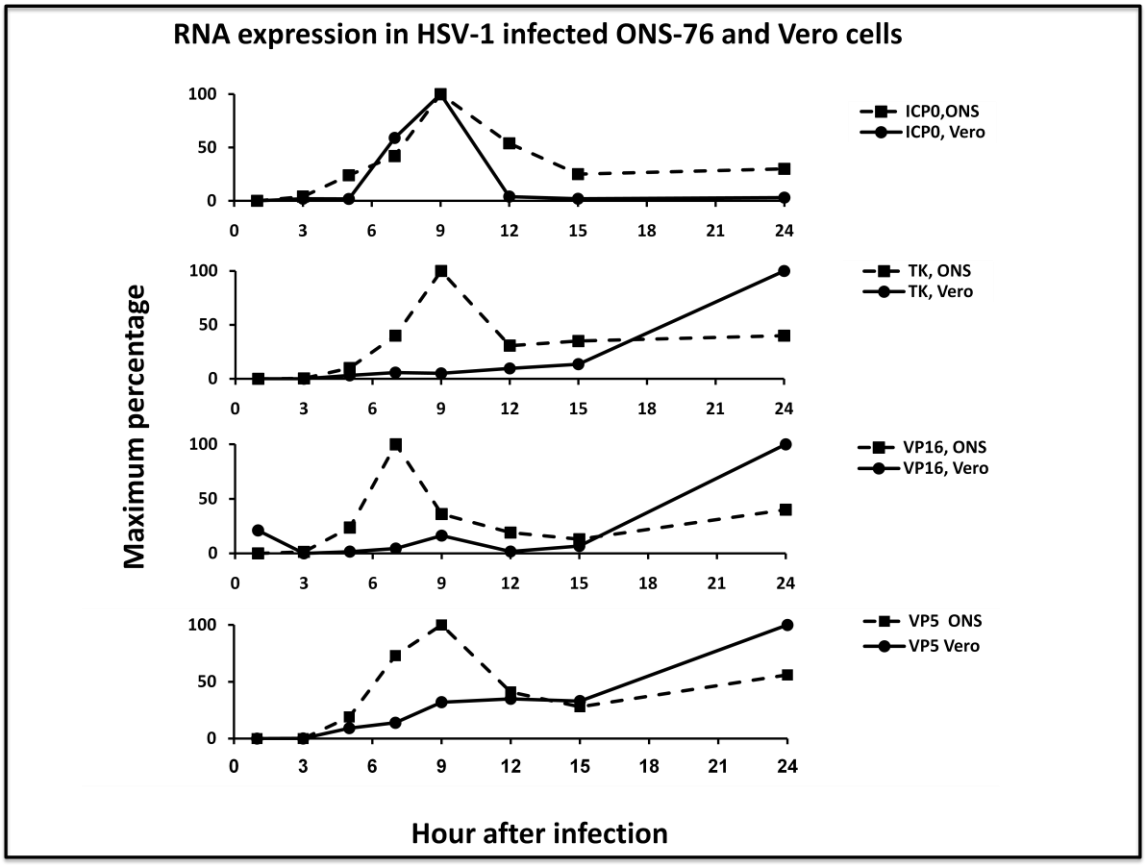

Figure 3.1.2. ICP0, TK, VP16 and VP5 genes expression in HSV-1 infected Vero and ONS-76 cells. Vero and ONS-76 cells were infected with HSV-1 at MOI of 5 pfu per cell. RNA was extracted from the samples harvested at 1, 3, 5, 7, 9, 12, 15 and 18 hours after infection. qRT PCR was used to examine the expression of ICP0, TK, VP16 and VP5 genes. Results are shown in the maximum percentage of fold changes in infected cells relative to mock-infected cells.

Cell type	Gene name	Fold change for the maximum percentage
Vero	ICP0	0.02×10^6
	TK	4.5×10^6
	VP16	184×10^6
	VP5	1.9×10^6
ONS-76	ICP0	0.02×10^6
	TK	0.35×10^6
	VP16	17×10^6
	VP5	0.18×10^6

Table 3.1. Fold change value of the maximum percentage for each gene transcript in figure 3.1.2.

After infection HSV-1 degrades host mRNA (16, 32)and also causes a decrease in the rates of transcription of host cellular genes (72). Since I used qRT PCR for analyzing the viral transcription and cellular housekeeping gene GAPDH was used to normalize, Ct values of GAPDH were monitored during 24 hours after HSV-1 infection using a fixed amount of input RNA. The level of GAPDH Ct values in both cells exhibited relatively little change in the first 12 hours after infection, about 2 cycles for Vero cells and less than 1 cycle for ONS-76 cells. The major changes were observed in the late hours after infection (about 24 hours after infection). I concluded this to mean that GAPDH Ct value during first 12 hours post infection, at which time most of the gene expression program for lytic infections has been completed, does not affect the final results (figure 3.1.3).

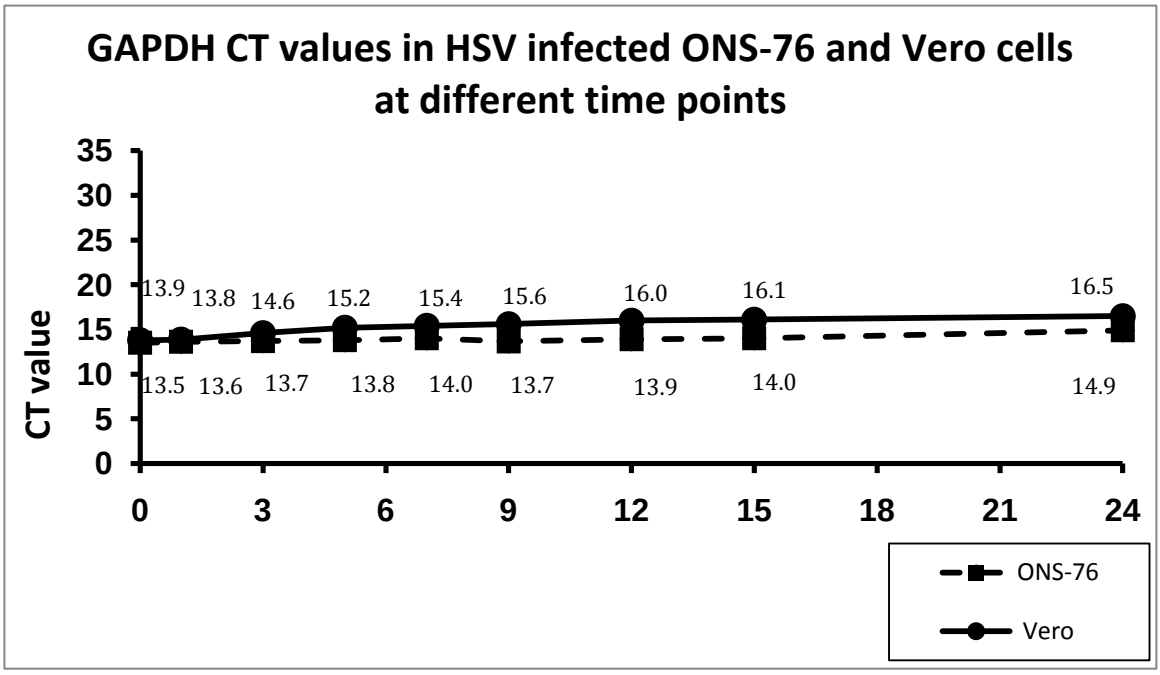

Figure 3.1.3. Effect of HSV-1 infection on GAPDH expression. Vero and ONS-76 cells were infected with HSV-1 at MOI of 5 pfu per cell. RNA was extracted from the harvested samples at 1, 3, 5, 7, 9, 12, 15 and 18 hours after infection. qRT PCR was used to evaluate the expression of GAPDH. Results are shown in Ct values.

It is known that, in contrast to E and L genes, the transcription of HSV-1 IE genes does not require de novo protein synthesis (reviewed in 66), and is not inhibited by protein synthesis inhibitor such as cyclohexamide (30). To determine if VP16 gene expression in ONS-76 cells followed the pattern of IE genes or L gene expression, both Vero and ONS-76 cells were infected with HSV-1 in the presence of cycloheximide and were harvested 7 hours after infection for ICP0, ICP27 (control for IE genes) and VP16 RNA.

Results showed that while synthesis of ICP0 was not affected by cyclohexamide, VP16 RNA was not synthesized in the presence of cycloheximide (figure 3.1.4), suggesting that the protein synthesis of early genes are required for VP16 expression and VP16 was regulated as an L or late gene in both ONS-76 and Vero cells.

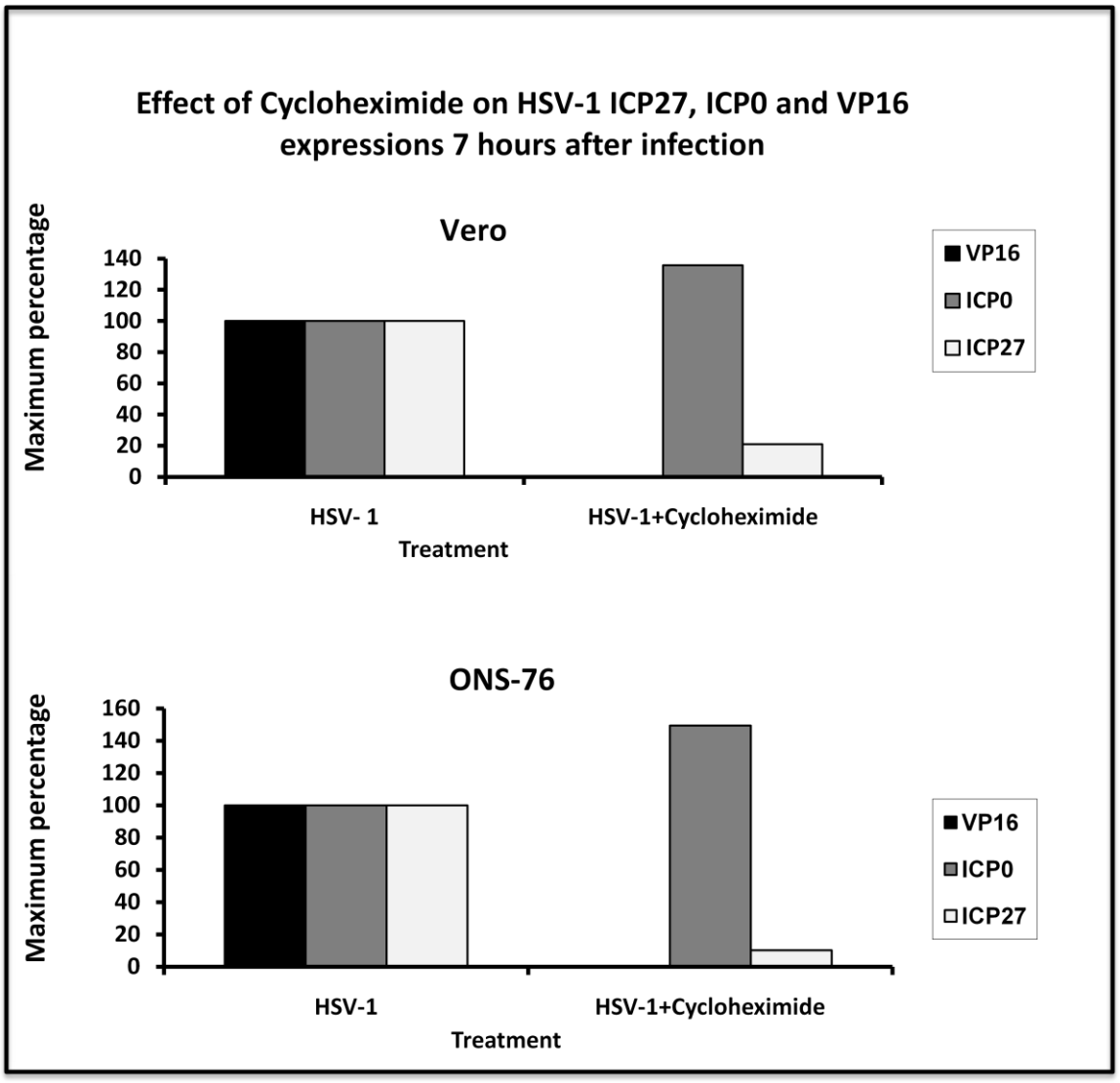

Figure 3.1.4. Cyclohexamide inhibits the expression of VP16 in both ONS-76 and Vero cells. Vero and ONS-76 cells were infected with HSV-1 and incubated in the presence of 12.5 μg/ml cylohexamide. Seven hours after infection cells were harvested for RNA and samples were evaluated for ICP0, ICP27 (IE transcript control) and VP16 expression with qRT PCR.

3.1.3. Viral protein synthesis in Vero and ONS-76 cells

Synthesis of HSV-1 ICP0, TK, VP16 and VP5 proteins in both cell lines was also examined 24 hours following infection with HSV-1. Vero and ONS-76 cells were infected with HSV at a MOI of 5 pfu per cell. Cells were harvested at 1, 3, 5, 7, 9, 12, 15 and 24 hours after infection and the cell lysates were subjected to Western blot analysis. While ICP0 and VP16 were detected in both cell lines, no TK or VP5 proteins were detected in ONS-76 cells (Fig 3.1.5). In the 65kDa area two close bands were detected and it was not clear which band was belonging to VP16. To identify the VP16 band, ONS-76 cells were transfected with plasmid pRG50 that expresses VP16 (positive control). Western blot of the transfected cells confirmed that the faster migrating band in ONS-76 cells was VP16 band while the slower migrating band was a nonspecific band, figure 3.1.5. The VP16 band in ONS-76 cells appeared earlier (5 hpi) than in Vero cells (9 hpi).

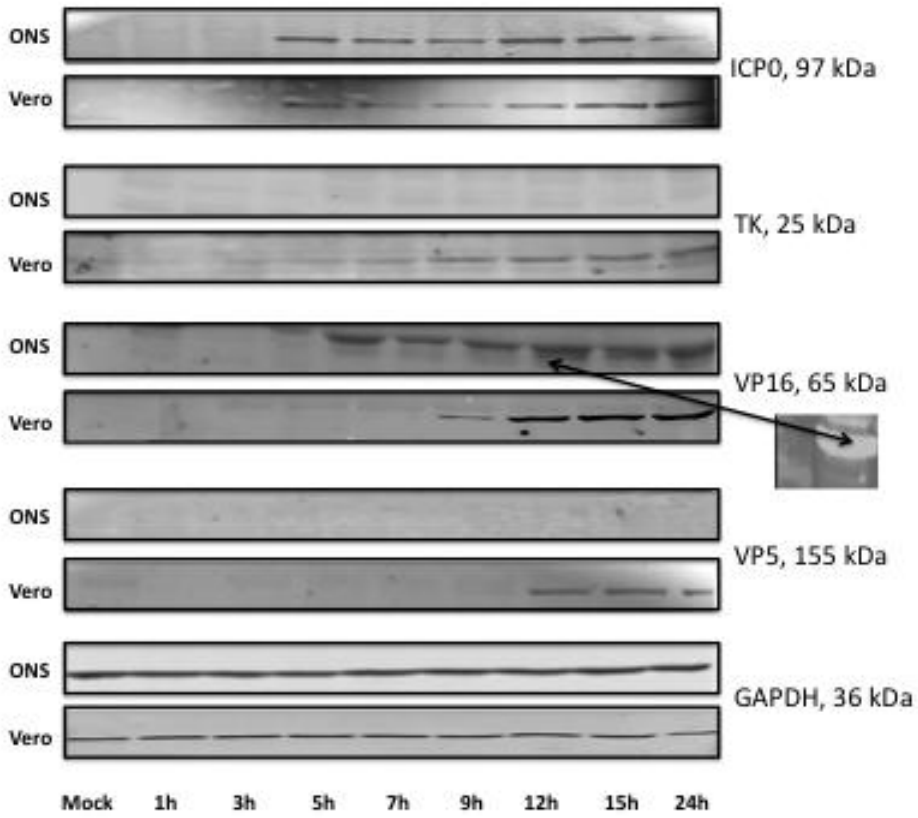

Figure 3.1.5. Kinetics of HSV-1 Protein synthesis in Vero and ONS-76 cells. Vero and ONS-76 cells were mock-infected or infected with HSV-1 and the cells were harvested at different time points after infection (1, 3, 5, 7, 9, 12, 15, 24 hours after infection). Cell lysates were subjected to western blot analysis using antibodies specific for ICP0, TK, VP16, VP5 and GAPDH. Although ICPO and VP16 were detected in both cell lines, TK and VP5 were not detected in ONS-76 cells Two bands were detected in the 65kDa area (VP16 expected area) in ONS-76 cells and it was not clear which band was the VP16. Transfected ONS-76 cells with plasmid pRG50 (VP16 expressing plasmid) revealed that the VP16 band is the lower band in ONS-76 cells. GAPDH was used as a loading control in both cell types.

3.2. UPR

3.2.1. Viability of cells following thapsigargin treatment

To study the effect of HSV-1 on the UPR, I activated the response with a calcium ionophore, thapsigargin. Thapsigargin is an ER stress inducer, which inactivates the ER **Ca** $^{2+}$ATPase resulting in depletion of Ca^{2+} from the ER lumen. To determine if this drug had an effect on the viability of cells cultures during the course of the experiment, Vero or ONS-76 cells, they were treated with either 100 nM thapsigargin or an equivalent volume of the drug solvent, DMSO. Cell viability was determined by a trypan blue dye exclusion assay 4 and 8 hours after treatment. Treated and untreated control cultures were dissociated with trypsin, mixed with trypan blue, and total and trypan blue staining cells counted. Thapsigargin demonstrated no discernible toxicity during 8 hours of treatment, figure 3.2.1.

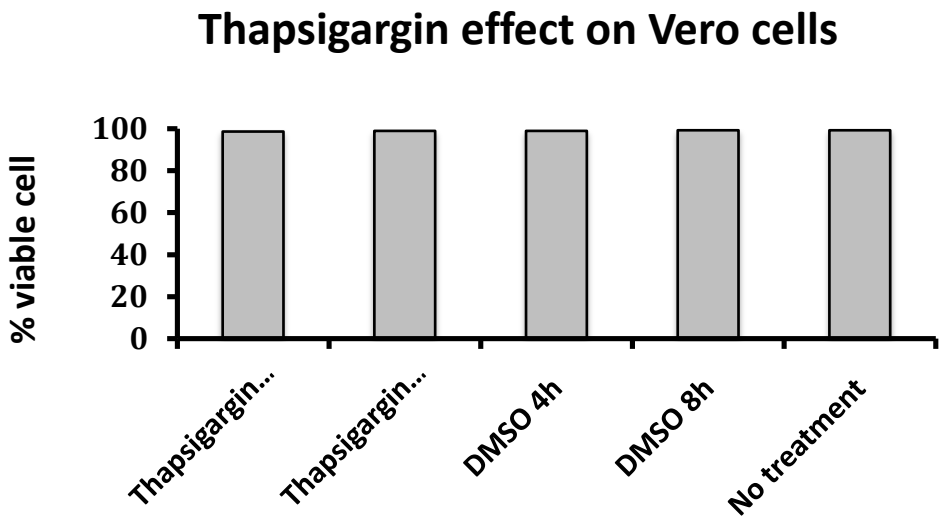

Figure 3.2.1. Thapsigargin and DMSO had no discernible cytotoxicity effect on Vero cells. Thapsigargin and DMSO treated cells were examined by trypan blue dye exclusion assay (The experimental procedure used is described in Material and Method Section).

3.2.2. Evaluate the efficiency of the primers designed to quantify the transcription of genes representative the three arms of UPR (IRE1, PERK, ATF6)

One approach for examining the UPR is to quantify the transcription of the genes representative of the three arms of UPR (IRE1, PERK and ATF6) by qRT-PCR. To do this, I designed sets of primers for transcripts of spliced XbpI, HERP, CHOP and BIP. Thapsigargin was used for experimental induction of UPR. Vero and ONS-76 cells were treated with thapsigargin for 4 hours and harvested for their RNA expression. All four primers detected the transcripts for UPR genes and these genes expression were increased in thapsigargin-treated Vero and ONS-76 cells, figure 3.2.2.

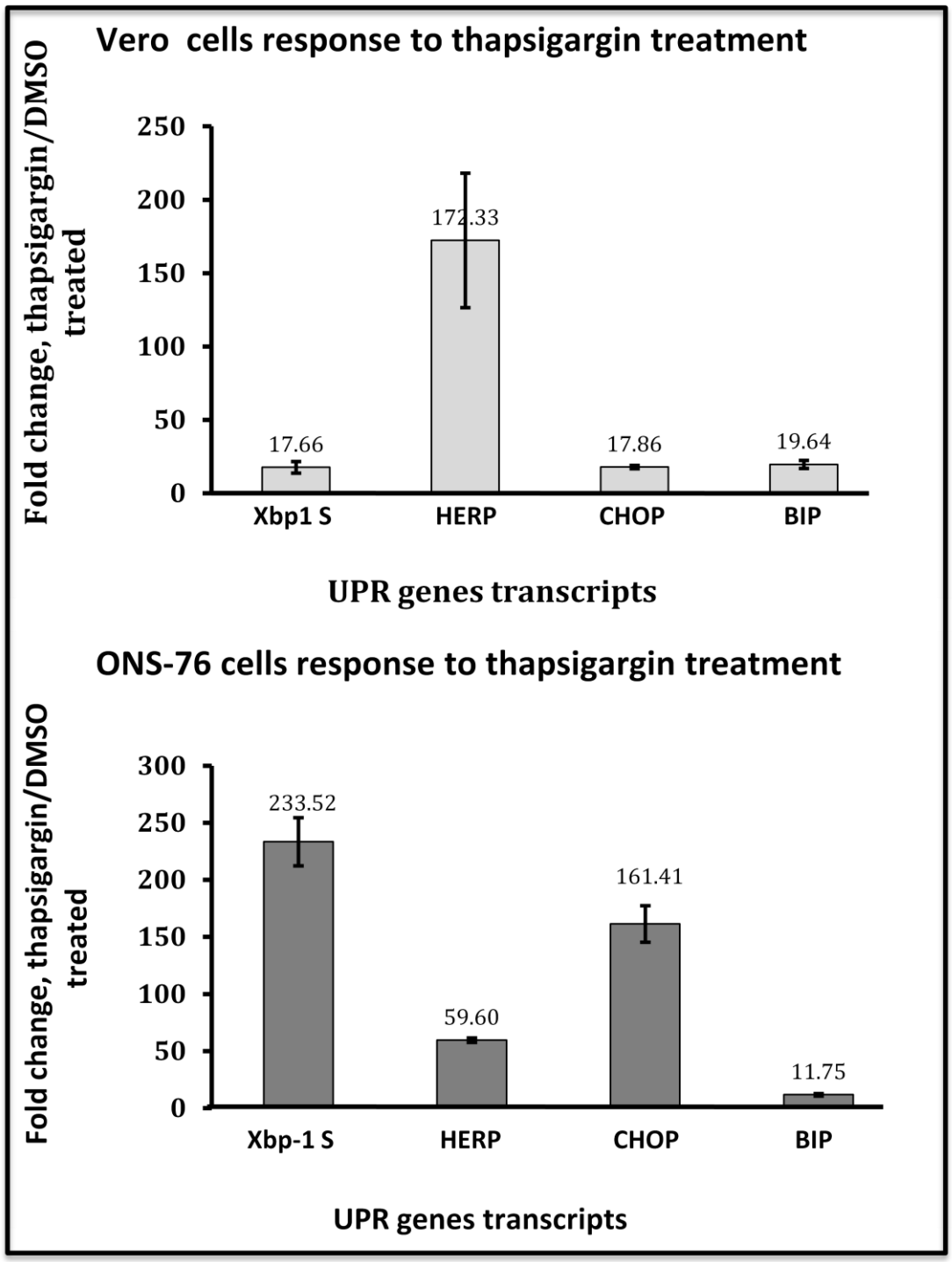

Figure 3.2.2 Expression of UPR- regulated genes in Vero and ONS cells in response to thapsigargin. Vero and ONS-76 cells were treated with 100nM thapsigargin for four hours. Cells were harvested and evaluated for their UPR transcripts expression with qRT-PCR. All four genes transcripts demonstrated an increase in expression in response to thapsigargin treatment. Error bars represent standard deviation.

3.2.3. HSV-1 induces the UPR

Many viruses have been observed to selectively regulate the UPR during replication, in particular, they induce arms of UPR which lead to expression of chaperones while preventing PERK and its suppression of global protein synthesis (see literature review). To investigate the regulation of the three arms of the UPR (IRE1, PERK and ATF6) during HSV-1 infection, Xbp-1, and its target gene HERP as well as CHOP and BIP the downstream target genes of PERK and ATF6 respectively were examined. RNA and protein samples of infected cells were collected at different time points post infection and analyzed for transcriptional and translation regulation of UPR components and their target genes by qRT-PCR and Western blotting. As can be observed in figure 3.2.3. a & b, the mRNA levels of Xbp-1 spliced and its downstream target gene, HERP were elevated in the HSV-1 infected cells in both Vero and ONS-76 cells. Xbp-1 mRNA splicing is associated with activation of the IRE1 pathway of UPR (reviewed in 23, 29). These results indicate that HSV-1 infection activates the IRE1 pathway in both cells leading to the splicing of Xbp-1 mRNA. While the transcript for CHOP, the gene down-stream from PERK was upregulated in ONS-76 cells, it was down regulated in Vero cells. BIP the ATF6 target gene only showed 3.45 fold change at 1 hour after infection only in ONS-76 cells but surprisingly showed no upregulation in either Vero or ONS-76 cells at 4 and 8 hours after infection. Altogether the results confirm that HSV-1 selectively activates the UPR pathways.

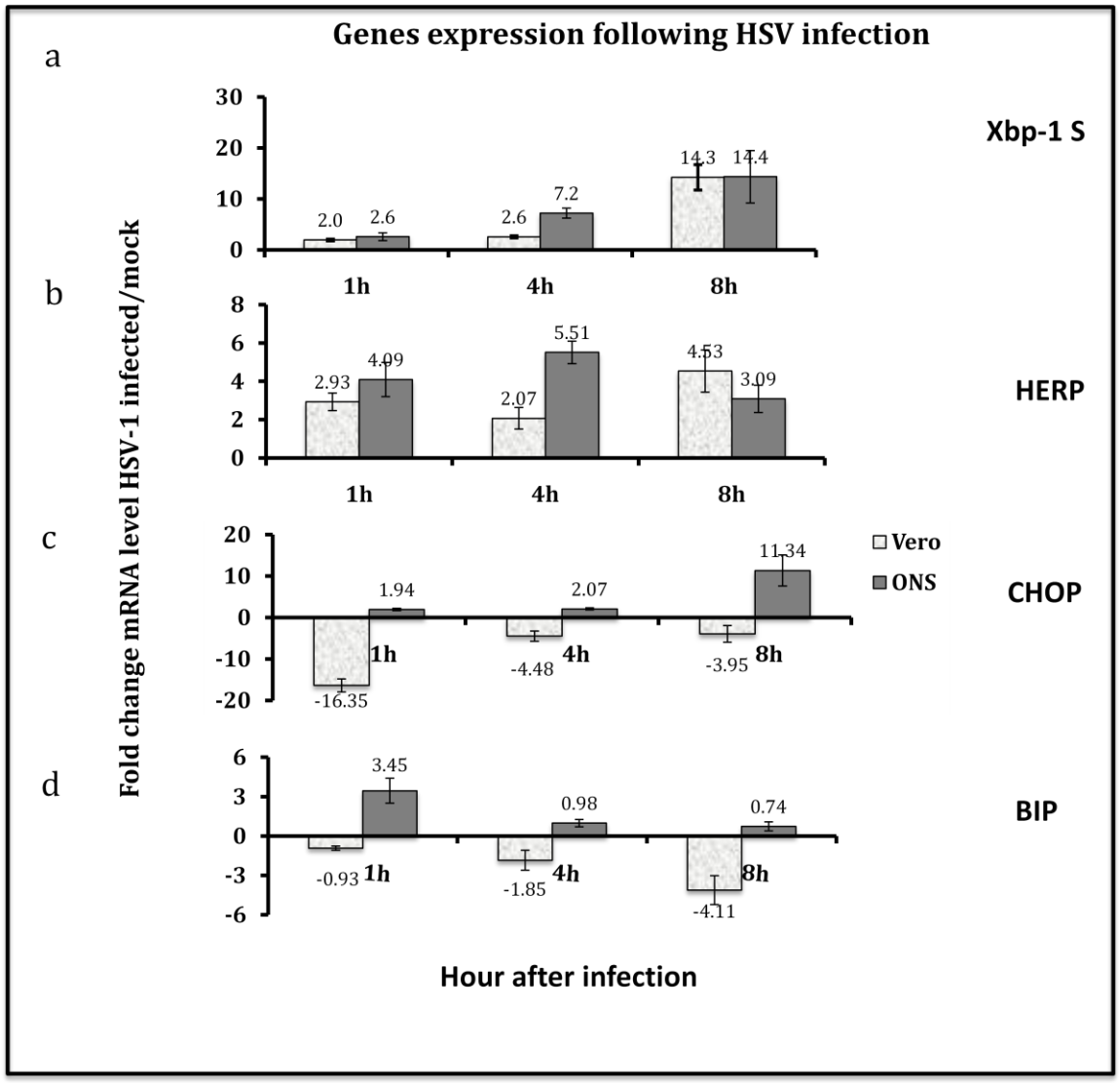

Figure 3.2.3. HSV-1 selectively activates the three arms of the UPR. Vero and ONS-76 were mock-infected or infected with HSV-1, cells harvested at different time points following infection and analyzed for UPR components and the transcripts of their target genes spliced Xbp-1, HERP, CHOP and BIP by qRT-PCR. (a & b) the mRNA levels for spliced Xbp-1 and its downstream target gene, HERP were elevated in the HSV-1 infected Vero and ONS-76 cells. (c) Transcripts for CHOP, the PERK downstream target were upregulated in ONS-76 cells, but down regulated in Vero cells. (d) BIP, the ATF6 target gene,not only showed no upregulation in either Vero or ONS-76 cells at 4 and 8 hours after infection but also showed down regulation in Vero cells at 8 hours.

3.2.4. HSV-1 infection does not inhibit eIF2α phosphorylation in Vero cells

The protein kinase PERK facilitates the translational control arm of the UPR by phosphorylation of eIF2α, a translation initiation factor that combines with GTP to escort initiator methionine-tRNA(i)(Met) to the ribosomal machinery during the initiation of protein synthesis. Phosphorylation of the alpha subunit of eIF2α on serine-51 inhibits global translation initiation, which reduces the influx of nascent polypeptides into the overloaded ER. eIF2α phosphorylation also facilitates the preferential translation of stress-related mRNAs, such as ATF4 which in turn activates the transcription of UPR genes. To investigate PERK-mediated signaling during HSV-1 infection further, I also analyzed the activation of eIF2α, which is phosphorylated by PERK following activation. Surprisingly, Western blot detected 38 kDa band suggesting eIF2α phosphorylation (p-eIF2α) at 3 hours after infection and continued to 22 hours in HSV-1 infected Vero cells. In contrast, no eIF2α phosphorylation was detected in ONS cells. Total eIF2α were detected in at the same density in all samples in both cells. 300nM thapsigargin treated cells was used as a positive control, figure 3.2.4.

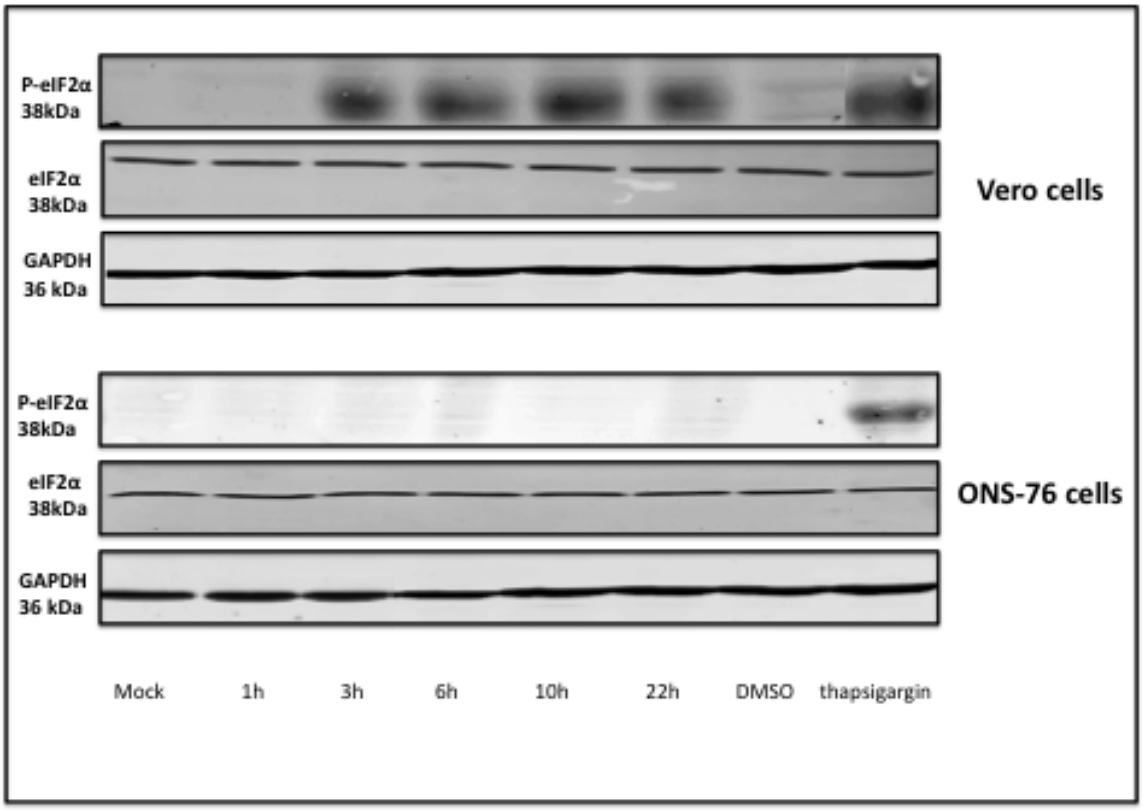

Figure 3.2.4. HSV-1 infection does not inhibit eIF2α phosphorylation in Vero cells but inhibits it in ONS-76 cells. Vero and ONS-76 cells were mock-infected or infected with HSV-1 at an MOI of 5 pfu per cell. At different time points post infection cells were harvested and lysates were prepared. Samples were then electrophoretically separated on 10 and 12% (p-eIF2α) polyacrylamide gels and transferred to nitrocellulose membranes. The membranes were sequentially probed with antibodies against p- eIF2α, total eIF2α and GAPDH (loading control). 300nM thapsigargin treated cells was used as positive control.

3.2.5. HSV-1 can selectively inactivate components of the UPR

After my observation on HSV-1 selective activation of the UPR and down regulation of CHOP and BIP (PERK and ATF6 target genes) in Vero cells, I examined if HSV-1 could selectively inactivate the activated components of the UPR. For this experiment, thapsigargin was used as a UPR inducer and DMSO as solvent control in Vero and ONS-76 cells, figure 3.2.5,a. Consistent with the previous experiment, induction of the UPR by thapsigargin treatment resulted in an increase in transcripts for spliced Xbp1, CHOP, HERP and BIP, figure 3.2.5, c. Next, I infected Vero and ONS-76 with HSV-1 after 4 hours treatment with thapsigargin. I harvested the cells 4 hours after infection for RNA transcripts, figure 3.2.5, b. HSV-1 infection caused a decrease in the expression of the UPR components. Expression of spliced Xbp1 and its target gene HERP in Vero cells dropped from 16.49 and 27.42 fold change to 7.98 and 2.86 fold change. Similarly, in ONS-76 cells, HSV-1 infection resulted in dramatic decrease in spliced Xbp1 and HERP expression and their fold change dropped from 52 to 1.37 and 0.92. HSV-1 infection caused a decrease in expression of CHOP and BIP and their fold change plunged to below zero in both cells, figure 3.2.5, d.

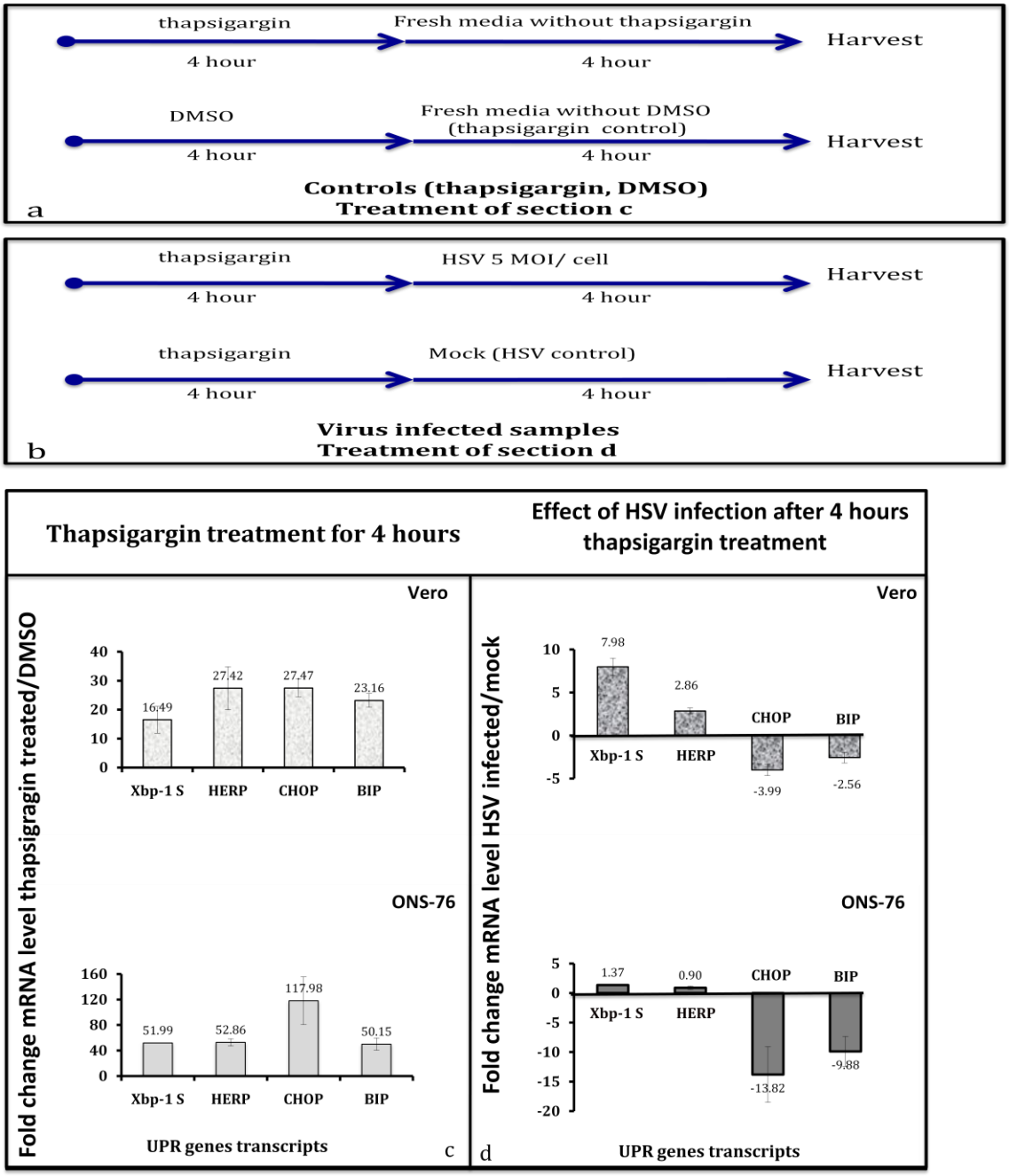

Figure 3.2.5. HSV-1 can selectively inactivate components of the UPR. (a and b) Experimental design. (a) Design for results in fig 3.2.5.c. Vero and ONS-76 cells were treated either with ER stressor, thapsigargin or DMSO (solvent control), after four hours media was replaced with fresh media without thapsigargin or DMSO, cells were harvested 4 hours later. (b) Design for results in fig 3.2.5.d. Media of thapsigargin treated cells after four hours were removed and cells were mock- infected or infected with HSV-1 and cells were harvested four hours after infection (c). Activation of UPR components by thapsigargin treatment for four hours. Expression of Xbp-1 S, HERP, CHOP and BIP were evaluated by qRT PCR. (d) Suppression of activated UPR components by HSV-1, Four hours after HSV-1 infection of thapsigargin treated cells, cells were harvested. qRT PCR was used to analyze the RNA expression of the samples.

3.2.6. Transient expression of ICP0 or VP16 does not increase Xbp1 spliced, CHOP and BIP expression

Previous experiments showed that not only could HSV-1 virus selectively activate the UPR but that it could also selectively inactivate activated components of the UPR. HSV-1 could specifically downregulate the CHOP and BIP in both cells. I was therefore interested in identifying the viral protein responsible for regulating the UPR. Since my experiments showed that HSV influences the UPR component early in infection, I examined the role of the IE gene ICP0 and VP16, transactivating tegument protein, which is enter the cells as component of virion.

Vero cells were transfected with plasmids CI-110, pRG50 that encode ICP0 and VP16 respectively or pcDNA3 (negative control) DNAs. Transfected cells were treated with either 100nM thapsigargin (ER stressor) or DMSO (solvent control) and then were harvested for RNA isolation. To evaluate the efficiency of transfection, Vero cells grown on cover slips, were transfected with the same plasmid DNAs and then were examined for fluorescence using antibody against ICP0 and VP16. Fluorescent staining showed about 7% of cells were positive for expression of ICP0 and VP16. When compared with the cells transfected with the control plasmid pcDNA3, in cells transfected to express ICP0 or VP16 there was no changes in UPR components (Xbp1 spliced, CHOP and BIP) activation, figure 3.2.6.

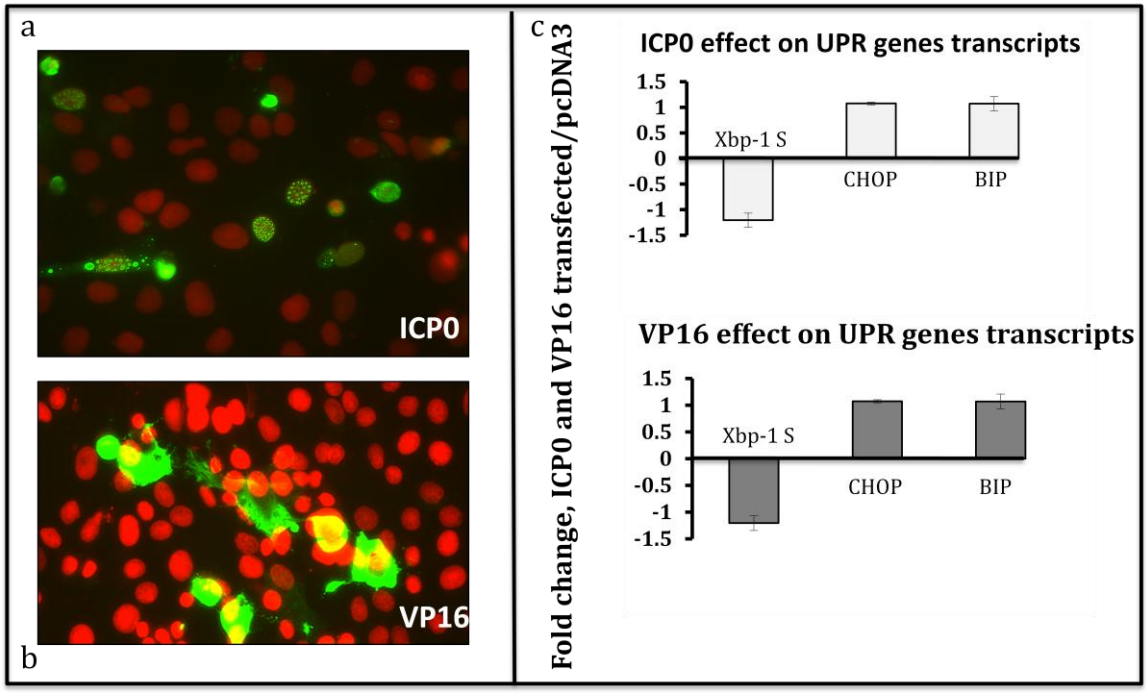

Figure 3.2.6. ICP0 and VP16 transient expression did not activate UPR components, Xbp-1 S, CHOP and BIP. Vero cells in six well tissue culture plate or on coverslips were transfected with 500ng DNA of CI-110 or pRG50 (plasmids expressing ICP0 and VP16) or pcDNA3 (empty plasmid as negative control). (a & b) immunofluorescent staining (explained in materials and methods) was used to evaluate the transfection efficiency and the expression of ICP0 and VP16. Trasfected cells in six well plates were treated with either 100nM thapsigargin (ER stressor) or DMSO (solvent control) for 4 hours and harvested with lysing buffer of RNeasy plus mini kit. Expression of Xbp-1 S, CHOP and BIP were evaluated by qRT PCR.

Chapter 4: Discussion

Viruses often induce host cells to produce large amount of viral proteins, many of which undergo glycosylation and other modifications in the ER, causing stress to the ER and consequently UPR activation. As a consequence of ER stress and induction of the UPR, protein synthesis is attenuated and under severe ER stress conditions the cell undergoes apoptosis; neither condition would be beneficial to the viral infection. However, other aspects of the UPR, such as the synthesis of chaperones, may be beneficial to the viral infection. Due to dependency of viruses on the host protein synthesis machinery, many viruses have evolved different mechanisms to selectively activate portion of the UPR that alleviate ER stress but counter the attenuation of the protein synthesis brought about by the activation of PERK.

In the present study, I tested the hypothesis that HSV-1 would selectively activate the IRE1 arm of the UPR, which leads to the synthesis of chaperones while suppressing PERK, which leads to the cessation of protein synthesis and ATF4-mediated apoptosis. I found that in Vero cells, in which infection with HSV-1 leads to a productive infection, the IRE1 induced transcripts for spliced Xbp1 and HERP were up-regulated while CHOP and Bip, regulated by PERK and ATF6, respectively, were down-regulated. In neuronal ONS-76 cells, while Bip transcripts were suppressed PERK transcripts were not. I also showed that HSV-1 could actively suppress both PERK and ATF6 activation induced by the drug thapsigargin.

Since viral events following HSV-1 infection of ONS-76 cells had never been described I compared the kinetics of various parameters of HSV-1 infection such as viral DNA synthesis, infectious virus production and, the mRNA transcription and protein synthesis of IE, E, and L genes during 24 hours after infection in Vero and human neuronal cells (ONS-76). In contrast to Vero cells, which are permissive for HSV-1 infection, ONS-76 cell seemed to be semi permissive to HSV-1 infection with limited viral DNA synthesis and infectious virus production. While in Vero cells the maximum level of viral DNA was 3.5 $x10^6$ genome equivalent per culture at 24h post infection, in ONS-76 the maximum level of viral DNA was $1.5x10^6$ genome equivalent at 9 hours and it dropped afterward to almost $3x10^5$ genome equivalent of DNA by 24 hpi, figure 3.1.1, b. The pattern of DNA synthesis in both cell types is consistent with the literature that

DNA replication occurs following expression of E genes, which is almost 5 to 7 hours post infection (reviewed in 66)

The pattern of infectious virus production in two cells was similar to the DNA synthesis. Infectious virus could not be detected in either Vero and ONS-76 cells in the first 4h after infection, but after 4h the rate of infectious viral replication increased and reached a peak of about $3.2x10^7$ pfu per culture at 12h in Vero cells. In contrast, the rate of increase in ONS-76 cells was slower and more modest with $2.8x10^6$ pfu per cell at 12 h. The higher level of viral replication and DNA synthesis in epithelial Vero cells was indicative of the permissive nature of Vero cells for the virus replication, and the limitation of DNA synthesis and viral replication in neuronal ONS-76 cells suggests that ONS-76 is semi permissive to HSV- 1 infection.

The kinetics of transcript and protein accumulation of representative viral genes for each temporal class (IE, E and L) in HSV-1 infected ONS-76 and Vero cells were also monitored. In Vero cells, the expression of viral genes at both the RNA (Figure 3.1.2) and protein (Figure 3.1.5) levels was consistent with the published literature (reviewed in 66, 82). Accumulation of ICP0 (IE) RNA and protein preceded TK (E), VP16 (L) and VP5 (L) expression. In contrast, in ONS-76 cells the transcripts from all temporal classes reached maximum levels at the time of IE expression in Vero cells. Furthermore, while TK and VP5 proteins were undetectable, VP16 protein could be detected as early as 5 hours after infection (9 hpi in Vero cells). Early expression of VP16 in ONS-76 cells might be related to the possible requirement for early VP16 expression during reactivation from latency in neurons (74).

Newly synthesized VP16, presumably induced by cellular transcription factors, has been shown to initiate reactivation from latency (76). I examined whether the expression of VP16 required viral IE gene products, as it does in permissive epithelial cells or whether the expression of VP16 induced by cellular factors independent of viral regulatory proteins. Although VP16 gene expression reached maximal levels at early hours of infection in ONS-76 cells, cyclohexamide treatment in HSV-infected cells prevented VP16 expression in ONS-76 cells, indicating that VP16 gene expression required prior protein synthesis in infected cells. This implies that either, like epithelial cells, VP16 expression required viral IE proteins, or it was dependent on cellular proteins made after infection.

Following HSV-1 infection, the transcript levels of spliced Xbp-1 and its downstream target gene, HERP were elevated in Vero and ONS-76 cells. Xbp-1 mRNA splicing is associated

with activation of IRE1 pathway of UPR (reviewed in 23, 29). These results indicate that HSV-1 infection activates the IRE1 pathway in both cells leading to the splicing of Xbp-1 RNA. Spliced Xbp-1 activates the expression of the UPR related genes involved in protein folding, protein entry to the ER, as well as genes encoding proteins involved in UPR mediated protein degradation, such as EDEM (ER degradation-enhancing α-mannosidase-like protein) and HERP, which lead to degradation of the unfolded proteins and reduction of the stress on the ER and consequently a more desirable environment for HSV-1 replication and virus survival. Lack of correlation among the levels of Xbp-1 spliced and HERP could be related to the other mechanisms involved in regulating HERP gene expression.

While CHOP, the PERK downstream gene transcript, was upregulated in ONS-76 cells, it was down regulated in Vero cells. CHOP is an apoptosis regulator and causes downregulation of the anti-apoptotic mitochondrial protein Bcl-2 (reviewed in 17) and finally death of infected cells, which is not beneficial to the virus. By inhibiting PERK activation, the virus might promote the survival of infected cells and more efficient viral replication in Vero cells. CHOP upregulation in ONS-76 cells might be due to the neuronal origin of these cells. Similar observations were made in West Nile virus infected neuroblastoma cells where induction of the proapoptotic protein CHOP leads to apoptosis and neuronal damage in neuroblastoma cells (59).

Another aspect of PERK activation is eIF2α phosphorylation, which causes protein synthesis attenuation. For this reason viruses such as HCMV (33), HCV (75) and adenovirus (37) have evolved mechanisms to prevent the accumulation of phosphorylated eIF2α and promote their protein synthesis. Surprisingly, I detected eIF2α phosphorylation (p-eIF2α 38 kDa band) in Vero cells at 3 hours after infection and this continued up to 22 hours post infection. In contrast, no eIF2α phosphorylation was detected in ONS cells. Lack of eIF2α phosphorylation fits with the CHOP upregulation, which was observed in HSV-1, infected ONS-76 cells. Numerous genes have been identified as down stream targets of CHOP, one of which is GADD34 (81). GADD34 has been shown to recruit PP1 to dephosphorylate eIF2α (61).

eIF2α is also phosphorylated by protein kinase R (PKR) which is activated by double-stranded RNA (dsRNA), ER stress, or amino acid deprivation, which often occurs during virus infection (25). Some viruses have evolved mechanisms to circumvent the resulting attenuation of translation, for instance a study by Wylie et al. has shown that HSV-2 antagonizes eIF2 phosphorylation through the action of the PKR antagonist ICP34.5, which redirects protein

phosphatase 1 (PP1) to dephosphorylate eIF2 during infection (84). The difference between my results in Vero cells and those in the literature may be related to the differences in HSV-1 virus and the cells used in the experiments.

Surprisingly, BIP, the ATF6 target gene showed no upregulation in either Vero or ONS-76 cells at 4 and 8 hours after infection. Since ATF6 pathway has an important role in increasing the ER chaperone capacity, quality control and ERAD, I expected to see an increase and not a decrease in its expression following HSV-1. This unexpected downregulation of BIP may be explained by the study which was done by Mao et al. (57); they demonstrated that the effect of HSV-1 on BIP expression is dependent on the strain of virus used. Cells infected with strain KOS showed no increase in BIP expression.

Altogether these results confirm that HSV-1 selectively activates the UPR pathways.

I investigated the affect of HSV-1 infection on the UPR activated in cells by thapsigargin. HSV-1 infection inactivated UPR components in Vero and ONS-76 cells, figure 3.2.5,a. Consistent with the previous experiment, HSV-1 infection resulted in a decrease in the expression of spliced Xbp1 transcripts and its target gene HERP in Vero cells and ONS-76 cells. Expression of CHOP and BIP in both cells were downregulated, figure 3.2.5, d.

Since my experiments showed that HSV influences the UPR early in infection, I examined the role of the IE gene, ICP0 and VP16 (a transactivating tegument protein) which is transported to infected cells as a component of virion. Comparing with pcDNA3, transient expression of ICP0 and VP16 in transfected Vero cells had almost no effect on UPR components (Xbp1 spliced, CHOP and BIP activation, figure 3.2.6. This suggests that these viral genes may not have a prominent role in regulating the UPR arms. An alternative explanation may be that, relatively few cells were transfected leading to the masking of the effects of the proteins by untransfected cells. Immunofluorescent analysis of the transfected cells indicated that only approximately 7% of cells expressed the viral proteins.

The goal of this study was to examine whether HSV-1 modulates the three arms of the UPR in epithelial (Vero) and neuronal (ONS-76) cells, the two cell types that represent the main sites for HSV productive replication and latency respectively. However, my results with ONS-76 cells should be interpreted with some caution. While these cells are believed to be neuronal in origin they may be very different from sensory neurons, the actual site of HSV latency. In contrast to differentiated sensory neurons ONS-76 cells were derived from undifferentiated

cerebellar neurons and grow actively. Another goal of this thesis was to determine the role of viral factors such as ICP0 and VP16 in UPR during HSV-1 infection. In my effort to determine if ICP0 and VP16 were responsible for suppressing aspects of the UPR I examined cells transfected with plasmids expressing the proteins. I found that neither plasmid had an effect on the genes representing the three arms of the UPR. This may be due to inefficient transfection of the cells by the plasmids. Therefore, to determine if the proteins were responsible for regulating the UPR I would compare the UPR in cells infected with wild-type HSV-1 and either ICP0 or VP16 viral mutants. The mutant V422 contains a deletion in the activation domain of VP16 but has a normal gene for ICP0 while mutant N212 has a defective gene for ICP0 but has normal VP16. Neither protein is required for inducing viral gene expression in u2os cells. Using viral mutants would allow me to infect all cells in a culture. The inability of either mutant to suppress components of the UPR in u2os cells would identify the protein as being responsible for the ability of HSV-1 to regulate the UPR.

References:

1. **Ambrose, R. L., and J. M. Mackenzie.** West nile virus differentially modulates the unfolded protein response to facilitate replication and immune evasion. J Virol **85:**2723-32.
2. **Amelio, A. L., P. K. McAnany, and D. C. Bloom.** 2006. A chromatin insulator-like element in the herpes simplex virus type 1 latency-associated transcript region binds CCCTC-binding factor and displays enhancer-blocking and silencing activities. J Virol **80:**2358-68.
3. **Brown, M. S., J. Ye, R. B. Rawson, and J. L. Goldstein.** 2000. Regulated intramembrane proteolysis: a control mechanism conserved from bacteria to humans. Cell **100:**391-8.
4. **Brush, M. H., D. C. Weiser, and S. Shenolikar.** 2003. Growth arrest and DNA damage-inducible protein GADD34 targets protein phosphatase 1 alpha to the endoplasmic reticulum and promotes dephosphorylation of the alpha subunit of eukaryotic translation initiation factor 2. Mol Cell Biol **23:**1292-303.
5. **Chan, S. W., and P. A. Egan.** 2005. Hepatitis C virus envelope proteins regulate CHOP via induction of the unfolded protein response. FASEB J **19:**1510-2.
6. **Chau, D. H., J. Yuan, H. Zhang, P. Cheung, T. Lim, Z. Liu, A. Sall, and D. Yang.** 2007. Coxsackievirus B3 proteases 2A and 3C induce apoptotic cell death through mitochondrial injury and cleavage of eIF4GI but not DAP5/p97/NAT1. Apoptosis **12:**513-24.
7. **Cheng, G., Z. Feng, and B. He.** 2005. Herpes simplex virus 1 infection activates the endoplasmic reticulum resident kinase PERK and mediates eIF-2alpha dephosphorylation by the gamma(1)34.5 protein. J Virol **79:**1379-88.
8. **Clements, G. B., and P. G. Kennedy.** 1989. Modulation of herpes simplex virus (HSV) infection of cultured neuronal cells by nerve growth factor and antibody to HSV. Brain **112 (Pt 5):**1277-94.

9. **de Haro, C., R. Mendez, and J. Santoyo.** 1996. The eIF-2alpha kinases and the control of protein synthesis. FASEB J **10:**1378-87.
10. **Decman, V., M. L. Freeman, P. R. Kinchington, and R. L. Hendricks.** 2005. Immune control of HSV-1 latency. Viral Immunol **18:**466-73.
11. **Deng, J., P. D. Lu, Y. Zhang, D. Scheuner, R. J. Kaufman, N. Sonenberg, H. P. Harding, and D. Ron.** 2004. Translational repression mediates activation of nuclear factor kappa B by phosphorylated translation initiation factor 2. Mol Cell Biol **24:**10161-8.
12. **Dever, T. E., L. Feng, R. C. Wek, A. M. Cigan, T. F. Donahue, and A. G. Hinnebusch.** 1992. Phosphorylation of initiation factor 2 alpha by protein kinase GCN2 mediates gene-specific translational control of GCN4 in yeast. Cell **68:**585-96.
13. **Efstathiou, S., and C. M. Preston.** 2005. Towards an understanding of the molecular basis of herpes simplex virus latency. Virus Res **111:**108-19.
14. **Farrell, M. J., A. T. Dobson, and L. T. Feldman.** 1991. Herpes simplex virus latency-associated transcript is a stable intron. Proc Natl Acad Sci U S A **88:**790-4.
15. **Favreau, D. J., M. Desforges, J. R. St-Jean, and P. J. Talbot.** 2009. A human coronavirus OC43 variant harboring persistence-associated mutations in the S glycoprotein differentially induces the unfolded protein response in human neurons as compared to wild-type virus. Virology **395:**255-67.
16. **Fenwick, M. L., and M. J. Walker.** 1978. Suppression of the synthesis of cellular macromolecules by herpes simplex virus. J Gen Virol **41:**37-51.
17. **Ferri, K. F., and G. Kroemer.** 2001. Organelle-specific initiation of cell death pathways. Nat Cell Biol **3:**E255-63.
18. **Fu, X., and X. Zhang.** 2002. Potent systemic antitumor activity from an oncolytic herpes simplex virus of syncytial phenotype. Cancer Res **62:**2306-12.
19. **Garber, D. A., P. A. Schaffer, and D. M. Knipe.** 1997. A LAT-associated function reduces productive-cycle gene expression during acute infection of murine sensory neurons with herpes simplex virus type 1. J Virol **71:**5885-93.
20. **Gething, M. J., and J. Sambrook.** 1992. Protein folding in the cell. Nature **355:**33-45.

21. **Gruenheid, S., L. Gatzke, H. Meadows, and F. Tufaro.** 1993. Herpes simplex virus infection and propagation in a mouse L cell mutant lacking heparan sulfate proteoglycans. J Virol **67:**93-100.

22. **GUROFF, G.** 1985. PC12 cells as amodel of neuronal differentiation in: Cell culture in the Neurosciences. Edited by J. E. Bottenstein and G. Sato. **New York: Plenum Press:**pp. 245-272.

23. **Harding, H. P., M. Calfon, F. Urano, I. Novoa, and D. Ron.** 2002. Transcriptional and translational control in the Mammalian unfolded protein response. Annu Rev Cell Dev Biol **18:**575-99.

24. **Harding, H. P., Y. Zhang, A. Bertolotti, H. Zeng, and D. Ron.** 2000. Perk is essential for translational regulation and cell survival during the unfolded protein response. Mol Cell **5:**897-904.

25. **He, B.** 2006. Viruses, endoplasmic reticulum stress, and interferon responses. Cell Death Differ **13:**393-403.

26. **He, B., M. Gross, and B. Roizman.** 1997. The gamma(1)34.5 protein of herpes simplex virus 1 complexes with protein phosphatase 1alpha to dephosphorylate the alpha subunit of the eukaryotic translation initiation factor 2 and preclude the shutoff of protein synthesis by double-stranded RNA-activated protein kinase. Proc Natl Acad Sci U S A **94:**843-8.

27. **Herr, W., R. A. Sturm, R. G. Clerc, L. M. Corcoran, D. Baltimore, P. A. Sharp, H. A. Ingraham, M. G. Rosenfeld, M. Finney, G. Ruvkun, and et al.** 1988. The POU domain: a large conserved region in the mammalian pit-1, oct-1, oct-2, and Caenorhabditis elegans unc-86 gene products. Genes Dev **2:**1513-6.

28. **Herrera, F. J., and S. J. Triezenberg.** 2004. VP16-dependent association of chromatin-modifying coactivators and underrepresentation of histones at immediate-early gene promoters during herpes simplex virus infection. J Virol **78:**9689-96.

29. **Hetz, C., and L. H. Glimcher.** 2009. Fine-tuning of the unfolded protein response: Assembling the IRE1alpha interactome. Mol Cell **35:**551-61.

30. **Honess, R. W., and B. Roizman.** 1974. Regulation of herpesvirus macromolecular synthesis. I. Cascade regulation of the synthesis of three groups of viral proteins. J Virol **14:**8-19.

31. **Hurtley, S. M., and A. Helenius.** 1989. Protein oligomerization in the endoplasmic reticulum. Annu Rev Cell Biol **5:**277-307.

32. **Inglis, S. C.** 1982. Inhibition of host protein synthesis and degradation of cellular mRNAs during infection by influenza and herpes simplex virus. Mol Cell Biol **2:**1644-8.

33. **Isler, J. A., A. H. Skalet, and J. C. Alwine.** 2005. Human cytomegalovirus infection activates and regulates the unfolded protein response. J Virol **79:**6890-9.

34. **Jiang, X., A. Alami Chentoufi, C. Hsiang, D. Carpenter, N. Osorio, L. Benmohamed, N. W. Fraser, C. Jones, and S. L. Wechsler.** The Herpes Simplex Virus Type 1 Latency-Associated Transcript Can Protect Neuron-Derived C1300 and Neuro2A Cells from Granzyme B-Induced Apoptosis and CD8 T-Cell Killing. J Virol **85:**2325-32.

35. **Jin, L., W. Peng, G. C. Perng, D. J. Brick, A. B. Nesburn, C. Jones, and S. L. Wechsler.** 2003. Identification of herpes simplex virus type 1 latency-associated transcript sequences that both inhibit apoptosis and enhance the spontaneous reactivation phenotype. J Virol **77:**6556-61.

36. **Kather, A., M. J. Raftery, G. Devi-Rao, J. Lippmann, T. Giese, R. M. Sandri-Goldin, and G. Schonrich.** Herpes simplex virus type 1 (HSV-1)-induced apoptosis in human dendritic cells as a result of downregulation of cellular FLICE-inhibitory protein and reduced expression of HSV-1 antiapoptotic latency-associated transcript sequences. J Virol **84:**1034-46.

37. **Katze, M. G., D. DeCorato, B. Safer, J. Galabru, and A. G. Hovanessian.** 1987. Adenovirus VAI RNA complexes with the 68 000 Mr protein kinase to regulate its autophosphorylation and activity. EMBO J **6:**689-97.

38. **Kaufman, R. J.** 2002. Orchestrating the unfolded protein response in health and disease. J Clin Invest **110:**1389-98.

39. **Kent, J. R., W. Kang, C. G. Miller, and N. W. Fraser.** 2003. Herpes simplex virus latency-associated transcript gene function. J Neurovirol **9:**285-90.

40. **Kieff, E. D., S. L. Bachenheimer, and B. Roizman.** 1971. Size, composition, and structure of the deoxyribonucleic acid of herpes simplex virus subtypes 1 and 2. J Virol **8:**125-32.

41. **Knipe, D. M., and A. Cliffe.** 2008. Chromatin control of herpes simplex virus lytic and latent infection. Nat Rev Microbiol **6:**211-21.

42. **Kristie, T. M., and P. A. Sharp.** 1990. Interactions of the Oct-1 POU subdomains with specific DNA sequences and with the HSV alpha-trans-activator protein. Genes Dev **4:**2383-96.

43. **Kristie, T. M., J. L. Vogel, and A. E. Sears.** 1999. Nuclear localization of the C1 factor (host cell factor) in sensory neurons correlates with reactivation of herpes simplex virus from latency. Proc Natl Acad Sci U S A **96:**1229-33.

44. **La Boissiere, S., T. Hughes, and P. O'Hare.** 1999. HCF-dependent nuclear import of VP16. EMBO J **18:**480-9.

45. **Lai, E., T. Teodoro, and A. Volchuk.** 2007. Endoplasmic reticulum stress: signaling the unfolded protein response. Physiology (Bethesda) **22:**193-201.

46. **Lei, K., A. Nimnual, W. X. Zong, N. J. Kennedy, R. A. Flavell, C. B. Thompson, D. Bar-Sagi, and R. J. Davis.** 2002. The Bax subfamily of Bcl2-related proteins is essential for apoptotic signal transduction by c-Jun NH(2)-terminal kinase. Mol Cell Biol **22:**4929-42.

47. **Li, B., B. Gao, L. Ye, X. Han, W. Wang, L. Kong, X. Fang, Y. Zeng, H. Zheng, S. Li, and Z. Wu.** 2007. Hepatitis B virus X protein (HBx) activates ATF6 and IRE1-XBP1 pathways of unfolded protein response. Virus Res **124:**44-9.

48. **Li, S., D. Carpenter, C. Hsiang, S. L. Wechsler, and C. Jones.** Herpes simplex virus type 1 latency-associated transcript inhibits apoptosis and promotes neurite sprouting in neuroblastoma cells following serum starvation by maintaining protein kinase B (AKT) levels. J Gen Virol **91:**858-66.

49. **Li, S., L. Ye, X. Yu, B. Xu, K. Li, X. Zhu, H. Liu, X. Wu, and L. Kong.** 2009. Hepatitis C virus NS4B induces unfolded protein response and endoplasmic reticulum overload response-dependent NF-kappaB activation. Virology **391:**257-64.

50. **Lillycrop, K. A., S. J. Dawson, J. K. Estridge, T. Gerster, P. Matthias, and D. S. Latchman.** 1994. Repression of a herpes simplex virus immediate-early promoter by the Oct-2 transcription factor is dependent on an inhibitory region at the N terminus of the protein. Mol Cell Biol **14:**7633-42.

51. **Lillycrop, K. A., C. L. Dent, S. C. Wheatley, M. N. Beech, N. N. Ninkina, J. N. Wood, and D. S. Latchman.** 1991. The octamer-binding protein Oct-2 represses HSV

immediate-early genes in cell lines derived from latently infectable sensory neurons. Neuron **7:**381-90.

52. **Livak, K. J., and T. D. Schmittgen.** 2001. Analysis of relative gene expression data using real-time quantitative PCR and the 2(-Delta Delta C(T)) Method. Methods **25:**402-8.
53. **Lodish, H. F.** 2004. Molecular cell biology.
54. **Luciano, R. L., and A. C. Wilson.** 2002. An activation domain in the C-terminal subunit of HCF-1 is important for transactivation by VP16 and LZIP. Proc Natl Acad Sci U S A **99:**13403-8.
55. **Ma, Y., and L. M. Hendershot.** 2004. ER chaperone functions during normal and stress conditions. J Chem Neuroanat **28:**51-65.
56. **Malhotra, J. D., and R. J. Kaufman.** 2007. The endoplasmic reticulum and the unfolded protein response. Semin Cell Dev Biol **18:**716-31.
57. **Mao, H., D. Palmer, and K. S. Rosenthal.** 2001. Changes in BiP (GRP78) levels upon HSV-1 infection are strain dependent. Virus Res **76:**127-35.
58. **McLennan, J. L., and G. Darby.** 1980. Herpes simplex virus latency: the cellular location of virus in dorsal root ganglia and the fate of the infected cell following virus activation. J Gen Virol **51:**233-43.
59. **Medigeshi, G. R., A. M. Lancaster, A. J. Hirsch, T. Briese, W. I. Lipkin, V. Defilippis, K. Fruh, P. W. Mason, J. Nikolich-Zugich, and J. A. Nelson.** 2007. West Nile virus infection activates the unfolded protein response, leading to CHOP induction and apoptosis. J Virol **81:**10849-60.
60. **Mulvey, M., C. Arias, and I. Mohr.** 2007. Maintenance of endoplasmic reticulum (ER) homeostasis in herpes simplex virus type 1-infected cells through the association of a viral glycoprotein with PERK, a cellular ER stress sensor. J Virol **81:**3377-90.
61. **Novoa, I., H. Zeng, H. P. Harding, and D. Ron.** 2001. Feedback inhibition of the unfolded protein response by GADD34-mediated dephosphorylation of eIF2alpha. J Cell Biol **153:**1011-22.
62. **Pasqual, G., D. J. Burri, A. Pasquato, J. C. de la Torre, and S. Kunz.** Role of the host cell's unfolded protein response in arenavirus infection. J Virol **85:**1662-70.

63. **Pavio, N., P. R. Romano, T. M. Graczyk, S. M. Feinstone, and D. R. Taylor.** 2003. Protein synthesis and endoplasmic reticulum stress can be modulated by the hepatitis C virus envelope protein E2 through the eukaryotic initiation factor 2alpha kinase PERK. J Virol **77:**3578-85.

64. **Peng, W., G. Henderson, M. Inman, L. BenMohamed, G. C. Perng, S. L. Wechsler, and C. Jones.** 2005. The locus encompassing the latency-associated transcript of herpes simplex virus type 1 interferes with and delays interferon expression in productively infected neuroblastoma cells and trigeminal Ganglia of acutely infected mice. J Virol **79:**6162-71.

65. **Preston, C. M.** 2000. Repression of viral transcription during herpes simplex virus latency. J Gen Virol **81:**1-19.

66. **Roizman B, K. D.** 2007. **Fields' virology**. **2**.

67. **Ron, D., and P. Walter.** 2007. Signal integration in the endoplasmic reticulum unfolded protein response. Nat Rev Mol Cell Biol **8:**519-29.

68. **Schroder, M., and R. J. Kaufman.** 2005. The mammalian unfolded protein response. Annu Rev Biochem **74:**739-89.

69. **Schubert, U., L. C. Anton, J. Gibbs, C. C. Norbury, J. W. Yewdell, and J. R. Bennink.** 2000. Rapid degradation of a large fraction of newly synthesized proteins by proteasomes. Nature **404:**770-4.

70. **Shen, J., X. Chen, L. Hendershot, and R. Prywes.** 2002. ER stress regulation of ATF6 localization by dissociation of BiP/GRP78 binding and unmasking of Golgi localization signals. Dev Cell **3:**99-111.

71. **Si, X., H. Luo, A. Morgan, J. Zhang, J. Wong, J. Yuan, M. Esfandiarei, G. Gao, C. Cheung, and B. M. McManus.** 2005. Stress-activated protein kinases are involved in coxsackievirus B3 viral progeny release. J Virol **79:**13875-81.

72. **Spencer, C. A., M. E. Dahmus, and S. A. Rice.** 1997. Repression of host RNA polymerase II transcription by herpes simplex virus type 1. J Virol **71:**2031-40.

73. **Tal-Singer, R., T. M. Lasner, W. Podrzucki, A. Skokotas, J. J. Leary, S. L. Berger, and N. W. Fraser.** 1997. Gene expression during reactivation of herpes simplex virus type 1 from latency in the peripheral nervous system is different from that during lytic infection of tissue cultures. J Virol **71:**5268-76.

74. **Tang, S., A. Patel, and P. R. Krause.** 2009. Novel less-abundant viral microRNAs encoded by herpes simplex virus 2 latency-associated transcript and their roles in regulating ICP34.5 and ICP0 mRNAs. J Virol **83:**1433-42.

75. **Tardif, K. D., K. Mori, and A. Siddiqui.** 2002. Hepatitis C virus subgenomic replicons induce endoplasmic reticulum stress activating an intracellular signaling pathway. J Virol **76:**7453-9.

76. **Thompson, R. L., C. M. Preston, and N. M. Sawtell.** 2009. De novo synthesis of VP16 coordinates the exit from HSV latency in vivo. PLoS Pathog **5:**e1000352.

77. **Umbach, J. L., M. F. Kramer, I. Jurak, H. W. Karnowski, D. M. Coen, and B. R. Cullen.** 2008. MicroRNAs expressed by herpes simplex virus 1 during latent infection regulate viral mRNAs. Nature **454:**780-3.

78. **Valyi-Nagy, J. M. E. G. T.** 2007. Latency strategies of herpesviruses.

79. **Vattem, K. M., and R. C. Wek.** 2004. Reinitiation involving upstream ORFs regulates ATF4 mRNA translation in mammalian cells. Proc Natl Acad Sci U S A **101:**11269-74.

80. **Wang, Q. Y., C. Zhou, K. E. Johnson, R. C. Colgrove, D. M. Coen, and D. M. Knipe.** 2005. Herpesviral latency-associated transcript gene promotes assembly of heterochromatin on viral lytic-gene promoters in latent infection. Proc Natl Acad Sci U S A **102:**16055-9.

81. **Wang, X. Z., M. Kuroda, J. Sok, N. Batchvarova, R. Kimmel, P. Chung, H. Zinszner, and D. Ron.** 1998. Identification of novel stress-induced genes downstream of chop. EMBO J **17:**3619-30.

82. **Weir, J. P.** 2001. Regulation of herpes simplex virus gene expression. Gene **271:**117-30.

83. **Wek, R. C., H. Y. Jiang, and T. G. Anthony.** 2006. Coping with stress: eIF2 kinases and translational control. Biochem Soc Trans **34:**7-11.

84. **Wylie, K. M., J. E. Schrimpf, and L. A. Morrison.** 2009. Increased eIF2alpha phosphorylation attenuates replication of herpes simplex virus 2 vhs mutants in mouse embryonic fibroblasts and correlates with reduced accumulation of the PKR antagonist ICP34.5. J Virol **83:**9151-62.

85. **Xuan, B., Z. Qian, E. Torigoi, and D. Yu.** 2009. Human cytomegalovirus protein pUL38 induces ATF4 expression, inhibits persistent JNK phosphorylation, and suppresses endoplasmic reticulum stress-induced cell death. J Virol **83:**3463-74.

86. **Yamada, M., K. Shimizu, K. Tamura, Y. Okamoto, Y. Matsui, S. Moriuchi, K. Park, E. Mabuchi, K. Yamamoto, T. Hayakawa, and et al.** 1989. [Establishment and biological characterization of human medulloblastoma cell lines]. No To Shinkei **41:**695-702.

87. **Ye, J., R. B. Rawson, R. Komuro, X. Chen, U. P. Dave, R. Prywes, M. S. Brown, and J. L. Goldstein.** 2000. ER stress induces cleavage of membrane-bound ATF6 by the same proteases that process SREBPs. Mol Cell **6:**1355-64.

88. **Yoshida, H., K. Haze, H. Yanagi, T. Yura, and K. Mori.** 1998. Identification of the cis-acting endoplasmic reticulum stress response element responsible for transcriptional induction of mammalian glucose-regulated proteins. Involvement of basic leucine zipper transcription factors. J Biol Chem **273:**33741-9.

89. **Yoshida, H., T. Matsui, A. Yamamoto, T. Okada, and K. Mori.** 2001. XBP1 mRNA is induced by ATF6 and spliced by IRE1 in response to ER stress to produce a highly active transcription factor. Cell **107:**881-91.

90. **Yura, Y., K. Terashima, H. Iga, Y. Kondo, T. Yanagawa, H. Yoshida, Y. Hayashi, and M. Sato.** 1987. Macromolecular synthesis at the early stage of herpes simplex virus type 2 (HSV-2) latency in a human neuroblastoma cell line IMR-32: repression of late viral polypeptide synthesis and accumulation of cellular heat-shock proteins. Arch Virol **96:**17-28.

91. **Zhang, H. M., X. Ye, Y. Su, J. Yuan, Z. Liu, D. A. Stein, and D. Yang.** Coxsackievirus B3 infection activates the unfolded protein response and induces apoptosis through downregulation of p58IPK and activation of CHOP and SREBP1. J Virol **84:**8446-59.

92. **Zheng, Y., B. Gao, L. Ye, L. Kong, W. Jing, X. Yang, and Z. Wu.** 2005. Hepatitis C virus non-structural protein NS4B can modulate an unfolded protein response. J Microbiol **43:**529-36.

93. **Zhou, Z. H., M. Dougherty, J. Jakana, J. He, F. J. Rixon, and W. Chiu.** 2000. Seeing the herpesvirus capsid at 8.5 A. Science **288:**877-80.

94. **Zinszner, H., M. Kuroda, X. Wang, N. Batchvarova, R. T. Lightfoot, H. Remotti, J. L. Stevens, and D. Ron.** 1998. CHOP is implicated in programmed cell death in response to impaired function of the endoplasmic reticulum. Genes Dev **12:**982-95.